



**HAL**  
open science

## Combinatorial boundary of a 3D lattice point set

Yukiko Kenmochi, Atsushi Imiya

► **To cite this version:**

Yukiko Kenmochi, Atsushi Imiya. Combinatorial boundary of a 3D lattice point set. *Journal of Visual Communication and Image Representation*, 2006, 17 (4), pp.738-766. 10.1016/j.jvcir.2005.11.001 . hal-00622083

**HAL Id: hal-00622083**

**<https://hal.science/hal-00622083>**

Submitted on 20 Feb 2013

**HAL** is a multi-disciplinary open access archive for the deposit and dissemination of scientific research documents, whether they are published or not. The documents may come from teaching and research institutions in France or abroad, or from public or private research centers.

L'archive ouverte pluridisciplinaire **HAL**, est destinée au dépôt et à la diffusion de documents scientifiques de niveau recherche, publiés ou non, émanant des établissements d'enseignement et de recherche français ou étrangers, des laboratoires publics ou privés.

# Combinatorial Boundary of a 3D Lattice Point Set

Yukiko Kenmochi <sup>a,\*</sup> Atsushi Imiya <sup>b</sup>

<sup>a</sup>*Department of Information Technology, Okayama University, Okayama, Japan*

<sup>b</sup>*Institute of Media and Information Technology, Chiba University, Chiba, Japan*

---

## Abstract

Boundary extraction and surface generation are important topological topics for three-dimensional digital image analysis. However, there is no adequate theory to establish relations between these different topological procedures in a completely discrete way. In this paper, we present a new boundary extraction algorithm which gives not only a set of border points but also a polyhedral surface whose vertices are border points by using the concepts of combinatorial/algebraic topologies. We show that our boundary can be considered to be a triangulation or polyhedrization of border points in the sense of general topology, that is, we clarify relations between border points and the surface structures.

*Key words:* boundary extraction, combinatorial surface, polyhedral complex

---

## 1 Introduction

Several algorithms have been presented for boundary extraction [4,19,20,31] and surface generation [4,6,8,17,22,24,32] of 3-dimensional digital images for purposes of visualization, calculation of geometric features such as surface areas, calculation of topological features such as Euler characteristics, numerical analysis for deformable objects, etc. Even if both topological objects, borders and surfaces, are required simultaneously (sometimes implicitly) for many applications as listed above, it is not easy to find a useful theory allowing to discuss both topological concepts for each point in a 3-dimensional lattice space, i.e. for each voxel in a 3-dimensional digital image. Note that there are many approximation techniques,

---

\* Corresponding author. Her current address is UMR 8049 - The Gaspard-Monge Institute, CNRS / University of Marne-la-Vallée / ESIEE, Marne-la-Vallée, France.  
E-mail addresses: y.kenmochi@esiee.fr (Y. Kenmochi), imiya@faculty.chiba-u.ac.jp (A. Imiya).

but we are interested in completely discrete techniques because our input are digital images and our computations for image analysis are also digital. Furthermore, such discrete techniques may bring us special geometric and topological properties which will be seen only in discrete spaces. The field of those studies are called discrete/digital geometry and topology [19] and useful properties may provide us new efficient algorithms for the applications listed above.

Even in the Euclidean space, it is not easy to draw relations between borders in the sense of general topology and surfaces in the sense of combinatorial topology [23]. More discussions on the historical backgrounds may be found in Section 2.

In this paper, we tackle a problem for clarifying relations between border points and surface points, i.e. points which are vertices of polyhedral surfaces, in a 3-dimensional lattice space. To solve the problem, we use polyhedral complexes such that all vertices are lattice points and the adjacent vertices are neighboring each other in the sense of 3-dimensional digital topology [19]. Such polyhedral complexes are called discrete polyhedral complexes and they enable us to give a topology or a polyhedral surface to a set of border points. By using discrete polyhedral complexes, we also present a new algorithm for extracting border points which constitute a polyhedral surface. We, therefore, succeed to extract border points and their surface structures simultaneously.

The definition of border points is based on general topology [9,23] and it has been shown that we can obtain border points by a set operation using neighborhoods [19,27,31] (see (8) in Section 2). Because we need to carry out the set operation for each point in a 3-dimensional lattice space, i.e. each voxel in a 3-dimensional digital image, the computational time is linear in the size of a digital image.

In two dimensions, some efficient border tracking algorithms have been proposed by using curve structures of border points [19,25] such that a set of border points is given as a sequence of points (or pixels) and each point (or pixel) has exactly two neighboring points (or pixels). Each border point is tracked by a “left-hand-on-wall” border following algorithm from the previous point in a sequence; therefore, we do not have to scan all points in a whole digital image; the computational time becomes linear in the number of border points.

In three dimensions, a completely different approach from that in two dimensions is commonly used because of the difficulty of finding “surface structures” of border points. An algebraic-topology based approach is taken so that unit cubes (or voxels) whose centroid are lattice points are first considered and then for border tracking the common faces between two voxels centered at points  $p$  in an object region and  $q$  in a complement of the region are considered [4]. Such faces are represented by an ordered pair  $(p, q)$ . Therefore, boundaries are represented by surfaces which are sets of square faces and whose topological structures are given as cellular complexes as shown in [20]. We can also consider the set of all points  $p$  of such pairs

$(p, q)$  as the border [31]. However, for such a set of points, we can not obtain any topological surface structures.

There are some axiomatic definitions of discrete surfaces such that all points of discrete surfaces are lattice points and not voxel faces [6,8,17,24]. However, the relations between border points and those surface points are not yet clarified; for example, we can find easily some border points which cannot be points of discrete surfaces defined in [6], called simplicity surfaces, as shown in Figure 1. Conversely, the connectedness of border points are shown in [16,18], but the concept of connectedness is clearly not sufficient for providing surface structures.

In order to give the relations between border points and surface points, we need a different approach. In the sense of combinatorial topology [3], this is a special formulation of a triangulation problem for border points. After presenting historical backgrounds in the next section, we define 3-dimensional discrete polyhedral complexes and give the combinatorial boundary which contains 2-dimensional surface structures in Section 3. In Section 4, we present an algorithm to provide a combinatorial boundary from any given 3-dimensional lattice point set. Because our algorithm is similar to a marching cubes algorithm [22,32] using a look-up table, our computational time is linear in the size of a 3-dimensional digital image. We then derive the relations between borders in the sense of general topology and our combinatorial boundaries. From these relations, we finally conclude that our combinatorial boundary extraction algorithm gives a triangulation for border points, simultaneously with border points, with respect to a given 3-dimensional lattice point set.

## 2 Historical Background

### 2.1 Borders, Frontiers and Combinatorial Boundaries

#### 2.1.1 Borders, Frontiers and Combinatorial Boundaries in $\mathcal{R}^n$

General topology studies topological spaces defined by open and closed sets [9,23], allowing to introduce interior  $Int(\mathbf{A})$ , border  $Br(\mathbf{A})$  and frontier<sup>1</sup>  $Fr(\mathbf{A})$  of a point set  $\mathbf{A}$ . We consider the topology in the  $n$ -dimensional Euclidean space  $\mathcal{R}^n$  introduced by the Euclidean distance:  $n$ -dimensional  $\varepsilon$ -neighborhoods

$$U_\varepsilon(x) = \{y \in \mathcal{R}^n : \|x - y\| < \varepsilon\} \quad (1)$$

<sup>1</sup> In [9], the term “boundary” is used instead of “frontier”. In this paper, we keep the term “boundary” for “combinatorial boundary” in the sense of combinatorial topology and follow the terminology in [23] to distinguish between boundaries in general topology and combinatorial topology.

of radius  $\varepsilon > 0$  define a basis of open sets for this Euclidean space.

If a point  $x$  in  $\mathbf{A} \subset \mathcal{R}^n$  is such that there exists a neighborhood  $\mathbf{U}_\varepsilon(x) \subseteq \mathbf{A}$ , then it is called an *interior point* of  $\mathbf{A}$ . Otherwise, a point  $x \in \mathbf{A}$  is called a *border point* of  $\mathbf{A}$ . Let  $Int(\mathbf{A})$  and  $Br(\mathbf{A})$  be the sets of all interior and border points such that

$$Int(\mathbf{A}) = \{x \in \mathbf{A} : \mathbf{U}_\varepsilon(x) \subseteq \mathbf{A}\}, \quad (2)$$

$$Br(\mathbf{A}) = \mathbf{A} \setminus Int(\mathbf{A}), \quad (3)$$

called the *interior* and *border* of  $\mathbf{A}$ , respectively. Then we have  $\mathbf{A} = Int(\mathbf{A}) \cup Br(\mathbf{A})$ .

Let  $\bar{\mathbf{A}}$  be the complement of  $\mathbf{A}$  such that  $\mathcal{R}^n = \mathbf{A} \cup \bar{\mathbf{A}}$ . Then, the interior points of  $\bar{\mathbf{A}}$  are also the *exterior points* of  $\mathbf{A}$ . The union of the borders of  $\mathbf{A}$  and  $\bar{\mathbf{A}}$  yields the *frontiers*  $Fr(\mathbf{A})$  and  $Fr(\bar{\mathbf{A}})$  such that

$$Fr(\mathbf{A}) = Br(\mathbf{A}) \cup Br(\bar{\mathbf{A}}) = Fr(\bar{\mathbf{A}}). \quad (4)$$

Figure 2 shows examples of the border and frontier of a point set  $\mathbf{A}$  in  $\mathcal{R}^2$ .

In this paper we also consider the *combinatorial boundary* of an  $n$ -dimensional polyhedral complex  $\mathbf{K}$  [3,23] so that we treat boundaries as  $(n - 1)$ -dimensional quasi-manifolds [21] as shown in Figure 1. If  $\mathbf{K}$  is a 3-dimensional polyhedral complex, then the combinatorial boundary  $\partial\mathbf{K}$  is the set of all 2-polyhedra  $\sigma$  of  $\mathbf{K}$  such that  $\sigma$  lies only in one 3-polyhedron of  $\mathbf{K}$ , together with all of its faces. The precise definitions of polyhedral complexes and combinatorial boundaries will be given in Section 3. Let  $\mathbf{K}$  be a 3-dimensional polyhedral complex which is a triangulated 3-manifold with boundary and  $|\mathbf{K}|$  be the union of the elements of  $\mathbf{K}$ , with the subspace topology induced by the topology of  $\mathcal{R}^n$ . Then, the relation between the frontier and the combinatorial boundary is derived such that

$$|\partial\mathbf{K}| = Fr(|\mathbf{K}|) \quad (5)$$

if  $|\mathbf{K}|$  is closed; see [23] for the proof.

### 2.1.2 Borders and Boundaries in $\mathcal{Z}^2$ and $\mathcal{Z}^3$

Let us consider the set  $\mathcal{Z}^n$  of all lattice points in  $\mathcal{R}^n$  such that their coordinates are all integers. For any point set  $\mathbf{V} \in \mathcal{Z}^n$ , which is given as an object component in an  $n$ -dimensional binary image, borders are also defined similarly to borders in  $\mathcal{R}^n$ . In this paper, we consider the cases  $n = 2, 3$ .

Traditionally, the following  $m$ -neighborhoods

$$\mathbf{N}_m(x) = \{y \in \mathcal{Z}^n : \|x - y\| \leq t\}$$

with  $t = 1, \sqrt{2}$  (resp.  $t = 1, \sqrt{2}, \sqrt{3}$ ) are in common used for  $x \in \mathbb{Z}^2$  (resp.  $x \in \mathbb{Z}^3$ ), and  $m = 4, 8$  (resp.  $m = 6, 18, 26$ ) stands for the cardinality of these neighborhood systems [19]. In distinction to  $\varepsilon$ -neighborhoods of (1), the radius  $t$  is only one of the three numbers  $1, \sqrt{2}$  or  $\sqrt{3}$ . It follows that these  $m$ -neighborhoods do not establish a basis of open sets of a topology on  $\mathbb{Z}^n$ , and that image analysis normally only assumes adjacency graphs in  $\mathbb{Z}^n$  for defining concepts of connectedness [19].

Let  $m \in \{4, 8\}$  for  $n = 2$  and  $m \in \{6, 18, 26\}$  for  $n = 3$ . If a point  $x$  in  $\mathbf{V} \subset \mathbb{Z}^n$  is such that  $\mathbf{N}_m(x) \subseteq \mathbf{V}$ , then  $x$  is called an *interior point*<sup>2</sup> (with respect to  $m$ -neighborhoods) [19,31]. The set of interior points of  $\mathbf{V}$  is called the *interior* of  $\mathbf{V}$  and denoted by

$$Int_m(\mathbf{V}) = \{x \in \mathbf{V} : \mathbf{N}_m(x) \subseteq \mathbf{V}\} \quad (6)$$

similarly to (2) for  $\mathbf{A} \subset \mathcal{R}^n$ . If a point  $x \in \mathbf{V}$  is not an interior point of  $\mathbf{V}$ , then  $x$  is called a *border point* of  $\mathbf{V}$  with respect to  $m$ -neighborhoods [19,31]. The set of all border points of  $\mathbf{V}$  is called the  *$m$ -border* of  $\mathbf{V}$ , denoted by

$$Br_m(\mathbf{V}) = \mathbf{V} \setminus Int_m(\mathbf{V}). \quad (7)$$

Equation (7) corresponds to (3).

In terms of mathematical morphology [27] it follows that an interior set  $Int_m(\mathbf{V})$  of (6) coincides with the erosion of  $\mathbf{V}$  with the structure element  $\mathbf{N}_m(o)$  where  $o$  is the origin of  $\mathbb{Z}^n$  [31]. We see that (7) also defines  $Br_m(\mathbf{V})$  via a set operation such as

$$Br_m(\mathbf{V}) = \{x \in \mathbf{V} : \mathbf{N}_m(x) \cap \bar{\mathbf{V}} \neq \emptyset\}. \quad (8)$$

This formulation is possible because the radii  $t$  of  $\mathbf{N}_m(x)$  is constant in  $\mathbb{Z}^n$ . In consequence, no set operation corresponding to (8) exists for  $Br(\mathbf{A})$  in  $\mathcal{R}^n$  of (3). Figure 3 shows examples of the 4-borders of  $\mathbf{V} \in \mathbb{Z}^2$  and of the complement  $\bar{\mathbf{V}}$ .

Let us consider the boundary points of  $\mathbf{V} \subset \mathbb{Z}^n$ , corresponding to the frontier points of  $\mathbf{A} \subset \mathcal{R}^n$ , in the sense of general topology. From (4), a point set  $\mathbf{A} \subset \mathcal{R}^n$  and the complement  $\bar{\mathbf{A}}$  has the frontier which is the “common boundary” as shown in Figure 2 (d). Similarly, we can define the  $m$ -boundary of  $\mathbf{V}$  as the union of the  $m$ -borders of  $\mathbf{V}$  and of  $\bar{\mathbf{V}}$ . Such  $m$ -boundaries are used for the composition of boundaries by contributions from both participating sets [22,26]. In digital image analysis, however,  $Br_m(\mathbf{V})$  and  $Br_m(\bar{\mathbf{V}})$  are considered separately [19,25,31] not only for

<sup>2</sup> We follow the terminology in [19], even if the term “inner point” is used instead of “interior point” in [31], to make a correspondence between interior points in  $\mathcal{R}^n$  and  $\mathbb{Z}^n$ .

boundary tracking but also for thinning<sup>3</sup>. They are called *internal and external  $m$ -boundaries*, respectively [27].

Such existence of “different boundaries” in a discrete space has been already pointed out by W. K. Clifford. In [5], he explained it using an example of a heap of white marbles on the top of which black marbles are put. The boundary of the white part would be a layer of white marbles and the boundary of the black part would be a layer of the black marbles, that is, the two adjacent parts have “different boundaries” when they are divided into two parts. He also referred to the Aristotelian definitions of continuity and discontinuity: the continuity as that of which two adjacent parts have the same boundary; and the discontinuity or discreteness as that of which two adjacent parts have different boundaries. Figure 3 (b) and (c) show examples of the internal 4-boundary  $Br_4(\mathbf{V})$  and the external 4-boundary  $Br_4(\bar{\mathbf{V}})$ , respectively.

This paper adopts the boundary approach as follows: the internal boundary, simply called  *$m$ -border*,  $Br_m(\mathbf{V})$  defines the initial point set, we consider the combinatorial boundary of an  $n$ -dimensional polyhedral complex  $\mathbf{K}$  such that all vertices are in  $Br_m(\mathbf{V})$ . We call such  $n$ -dimensional polyhedral complexes *discrete polyhedral complexes* to distinguish them with other (general) polyhedral complexes. This is a special formulation of a triangulation problem for  $Br_m(\mathbf{V})$  in the sense of combinatorial topology [3]. In the following sections, we give definitions which are necessary for construction of discrete polyhedral complexes and present a solution for the triangulation problem. We afterwards derive the relations between  $Br_m(\mathbf{V})$  and the combinatorial boundary of a discrete polyhedral complex  $\partial\mathbf{K}$  with respect to the relation of (5) for  $\mathcal{R}^n$  (see Theorem 6 and Corollary 7 in Section 5).

## 2.2 Border Tracking and Surface Representation in $\mathbb{Z}^n$

### 2.2.1 Connectedness of Borer Points and Border Tracking

A set  $\mathbf{B} \subset \mathbb{Z}^n$  is said to be *connected or  $m$ -connected* if any pair of  $x, y \in \mathbf{B}$  has a point sequence  $x_1 = x, x_2, \dots, x_k = y$  such that all  $x_i \in \mathbf{B}$  and  $x_{i+1} \in N_m(x_i)$  [19].

In  $\mathbb{Z}^2$ , it is known that the  $m$ -border  $Br_m(\mathbf{V})$  of  $\mathbf{V} \subset \mathbb{Z}^2$  is  $m'$ -connected if  $\mathbf{V}$  is  $m'$ -connected without hole where  $(m, m') = (4, 8), (8, 4)$  [19, 25]. All  $m$ -border points are then tracked as a sequence of points such as  $x_1, x_2, x_3, \dots$  and every point  $x_i$  in the sequence is found as an element of  $m'$ -neighborhood of the previous point  $x_{i-1}$  [19]. We see in this approach that the definition of a “curve” is implicitly given as

---

<sup>3</sup> For thinning of  $\mathbf{V} \subset \mathbb{Z}^n$ , we consider simple points which we can remove without collapsing the criteria of digital topology [19]. Obviously, simple points are related to border/boundary points of  $\mathbf{V} \subset \mathbb{Z}^n$ .

a sequence of points. In other words, border points are tracked by using the “curve structures” in  $\mathcal{Z}^2$ .

In  $\mathcal{Z}^3$ , it has been shown in [16,18] that the  $m$ -border  $Br_m(\mathbf{V})$  of  $\mathbf{V} \subset \mathcal{Z}^3$  is  $m'$ -connected if  $\mathbf{V}$  and  $\bar{\mathbf{V}}$  are  $m'$ - and  $m$ -connected respectively for any pair  $(m, m') \in \{6, 18, 26\} \times \{6, 18, 26\} \setminus (6, 6)$ .<sup>4</sup> Similarly to the case of two dimensions, for border tracking of  $\mathbf{V}$  in  $\mathcal{Z}^3$ , we need a definition of a “surface” instead of that of a “curve” in  $\mathcal{Z}^2$ . Clearly, the connectivity is not enough for representing the structures of surfaces such as triangulated surfaces.

### 2.2.2 Surface Representation in $\mathcal{Z}^3$

The definition of “surfaces” in  $\mathcal{Z}^3$  is more complicated than that of “curves” in  $\mathcal{Z}^2$ . There exist various definitions of two-dimensional surfaces in  $\mathcal{Z}^3$ . The approaches are mainly classified into the following four types:

- (1) the graph-theory based approach: a surface is defined as a set of lattice points which satisfies some conditions based on the neighborhood relations or the connectedness [6,24,31]. Every point on surfaces is considered to have a characteristic of spatial separation according to the Jordan surface theorem in a local sense.
- (2) the algebraic-topology based approach: surfaces are defined as the combinatorial boundaries of 3-dimensional cellular complexes. In [4,10,20], cells are considered to be unit cubes (or voxels) whose centroids correspond to lattice points and surfaces are represented by sets of faces of unit cubes. In [11], simplicial complexes are used instead of cellular complexes so that the vertices of simplexes are all lattice points.
- (3) the combinatorial-manifold based approach: surfaces are triangulated and any point on a surface is topologically equivalent to the central point of an open disc [6,8,17].
- (4) the analytical approach: geometric surfaces such as planes and spheres are defined by using inequalities in  $\mathcal{Z}^3$  instead of using equations in  $\mathcal{R}^3$  [1,2,7].

The analytical approach can be applied if only geometric objects such as planes and spheres are considered. In this paper, we would like to treat any free-form objects. Thus, we cannot take the analytical approach.

The graph-theory based approach is the most classic, but is also axiomatic. Since it contains only neighborhood relations and not topological structures, the combinatorial-manifold based approach has been taken in [6,17] for making comparison between the graph-theory based approach and the combinatorial-manifold based approach. Clearly, the combinatorial-manifold based approach has the strong power for inves-

<sup>4</sup> This holds if a digital picture space  $(\mathcal{Z}^3, m', m)$  is weakly normal, i.e. it has one of such pairs  $(m, m')$  from Proposition 7.4.1 in [18].



tracking topological structures, but it is not evident that a set of border points can become a combinatorial manifold. For example, a set of border points may not construct a manifold as shown in Figure 1 (b) and (c); they are called quasi-manifolds [21] and (b) is also called a pseudo-manifold [28].

For border tracking in  $\mathcal{Z}^3$ , therefore, the algebraic-topology based approach based on voxels is commonly used [4] such as tracking the common faces between two voxels centered at the points  $p$  in  $\mathbf{V} \subset \mathcal{Z}^3$  and  $q$  in  $\bar{\mathbf{V}} = \mathcal{Z}^3 \setminus \mathbf{V}$ . Such faces are represented by the ordered pair  $(p, q)$ . Since  $q \in \mathbf{N}_6(p) \cap \bar{\mathbf{V}}$ , the set of all  $p$  of such pairs  $(p, q)$  becomes equal to  $Br_6(\mathbf{V})$  of (8). In this approach, the “surface” is represented by a set of square faces of voxels and the topological structures of cellular complexes, i.e. voxels, voxel faces, etc., are shown in [20].

Because we would like to consider triangulated surfaces on the points of  $Br_m(\mathbf{V})$ , we need another notion based on algebraic topology. In this paper, we extend our notions of discrete simplexes in [11] to discrete convex polyhedra and give the definition of discrete polyhedral complexes instead of discrete simplicial complexes in [11]. The following sections are devoted for presenting triangulation of  $Br_m(\mathbf{V})$ .

### 3 Discrete Polyhedral Complexes and Combinatorial Boundaries

In this section, we give definitions of a polyhedral complex which consists of a finite set of convex polyhedra such that the vertices are all points in  $\mathcal{Z}^3$  and any adjacent vertices are  $m$ -neighboring. Given a lattice point set  $\mathbf{V} \subset \mathcal{Z}^3$ , such a polyhedral complex is introduced for giving a complicial representation, i.e. an object representation by a complex, of  $\mathbf{V}$ . An algorithm for obtaining a polyhedral complex from  $\mathbf{V}$  will be presented in the next section. Similar complicial representations for  $\mathbf{V}$  are also found, for examples, in [14,18,29]. The differences between our complicial representation and them will be discussed in Section 6.

#### 3.1 Convex Polyhedra and Polyhedral Complexes in $\mathcal{R}^n$

For the definitions of convex polyhedra and polyhedral complexes in  $\mathcal{R}^n$ , we follow the notions in [33].<sup>5</sup> Similar notations are also seen in [3,28].

**Definition 1** *A convex polyhedron  $\sigma$  is the convex hull of a finite set of points in some  $\mathcal{R}^d$ .*

The dimension of a convex polyhedron  $\sigma$  is the dimension of its affine hull. An  $n$ -dimensional convex polyhedron  $\sigma$  is abbreviated to an  $n$ -polyhedron. For in-

<sup>5</sup> Instead of the term “convex polyhedra”, “polytopes” is used in [33]

stance, a point is a 0-polyhedron, a line segment is a 1-polyhedron, a triangle is a 2-polyhedron, and a tetrahedron is a 3-polyhedron. A linear inequality  $a \cdot x \leq z$  is valid for  $\sigma$  if it is satisfied for all points  $x \in \sigma$ . A *face* of  $\sigma$  is then defined by any set of the form

$$\delta = \sigma \cap \{x \in \mathcal{R}^d : a \cdot x = z\}$$

where  $a \cdot x \leq z$  is valid for  $\sigma$ . For instance, a 3-polyhedron which is a tetrahedron has four 0-polyhedra, six 1-polyhedra and four 2-polyhedra for its faces. The point of a 0-polyhedron, the endpoints of a 1-polyhedron and the vertices of 2- and 3-polyhedra are called the *vertices* of each convex polyhedron.

**Definition 2** A *polyhedral complex*  $\mathbf{K}$  is a finite collection of convex polyhedra such that

- (1) the empty polyhedron is in  $\mathbf{K}$ ,
- (2) if  $\sigma \in \mathbf{K}$ , then all faces of  $\sigma$  are also in  $\mathbf{K}$ ,
- (3) the intersection  $\sigma \cap \tau$  of two convex polyhedra  $\sigma, \tau \in \mathbf{K}$  is a face both of  $\sigma$  and of  $\tau$ .

The dimension of  $\mathbf{K}$  is the largest dimension of a convex polyhedron in  $\mathbf{K}$ .

Note that any  $\mathbf{K}$  is a partially ordered set which can be identified with a topological space called a discrete space; the proof is found in Section 6.1 of [3].

### 3.2 Discrete Convex Polyhedra and Discrete Polyhedral Complexes

Now we consider polyhedral complexes such that the vertices of convex polyhedra are all lattice points in  $\mathcal{Z}^3$  and the adjacent vertices are  $m$ -neighboring for  $m = 6, 18, 26$ . For constructing such polyhedral complexes, we first consider all possible convex polyhedra such that all vertices are lattice points and any adjacent vertices of a convex polyhedron are  $m$ -neighboring each other for  $m = 6, 18, 26$ . Such convex polyhedra and polyhedral complexes are called *discrete convex polyhedra* and *discrete polyhedral complexes* hereafter. The constraints allow us to look for a discrete convex polyhedron which is not larger than the unit cubic region as follows.

Let us consider all possible convex polyhedra in a unit cubic region such that the vertices of each convex polyhedron are the vertices of a unit cube. A unit cube has eight lattice points for the vertices. For each lattice point we assign the value of either 1 or 0 and call the point a 1- or 0-point, respectively. There are 256 configurations of 1- and 0-points for the eight lattice points in a unit cubic region. In fact, we can reduce the number of the configurations from 256 to 23 with considering

the congruent configurations by rotations as shown in Table 1.<sup>6</sup>

For each configuration, we obtain a convex polyhedron such that the vertices of the polyhedron are 1-points. We then classify each convex polyhedron into a set of discrete convex polyhedra with the dimension of  $n = 0, 1, 2, 3$  and with the  $m$ -neighborhood relations between the adjacent vertices for  $m = 6, 18, 26$  as shown in Table 2. From Table 2, we see that there are a finite number of discrete convex polyhedra for each neighborhood system and for each dimension from 0 to 3. For the abbreviation, we call the  $n$ -dimensional discrete convex polyhedra in Table 2 *discrete  $n$ -polyhedra* hereafter.

For any neighborhood system, an isolated point of configuration P1 in Table 2 is regarded as a discrete 0-polyhedron. Similarly, the line segment for configuration P2a is regarded as a discrete 1-polyhedron for any neighborhood system because the adjacency between two points are  $m$ -neighboring for any  $m = 6, 18, 26$ . However, the line segment of configuration P2b is not considered to be a discrete 1-polyhedron for the 6-neighborhood system, but considered to be a discrete 1-polyhedron for the 18- and 26-neighborhood systems. The line segment of configuration P2c is considered to be a discrete 1-polyhedron only for the 26-neighborhood system. Table 2 illustrates that we have one, two and three of discrete 1-polyhedra for the 6-, 18- and 26-neighborhood systems, respectively. A discrete 2-polyhedron is always bounded by discrete 1-polyhedra which are the faces of the discrete 2-polyhedron. Therefore, all discrete 2-polyhedra for the 6-neighborhood system have the point configuration of P4a. For the 18- and 26-neighborhood systems, four and five different discrete 2-polyhedra are considered, respectively. In a similar way, a discrete 3-polyhedron is bounded by discrete 2-polyhedra which are the faces of the discrete 3-polyhedron. The discrete 3-polyhedra for each neighborhood system are illustrated in the last line of Table 2.

In Table 2, we see that for each  $m$ -neighborhood system,  $m = 6, 18, 26$ , every  $n'$ -dimensional face of any discrete  $n$ -polyhedron for  $n' < n$  is also a discrete  $n'$ -polyhedron. This is important because it enables us to construct a discrete polyhedral complex which is a finite collection of discrete convex polyhedra satisfying the three conditions in Definition 2 for each  $m$ -neighborhood system. Hereafter, we call an  $n$ -dimensional discrete polyhedral complex, for short, a *discrete  $n$ -complex*.

If we cannot decompose a discrete  $n$ -polyhedron into other discrete  $n$ -polyhedra in one of the neighborhood systems, such a discrete  $n$ -polyhedron also called a *discrete  $n$ -simplex* [11]. In  $\mathcal{R}^3$ , any  $n$ -dimensional simplex has  $n + 1$  vertices [3] while there exist, in  $\mathcal{Z}^3$ , discrete  $n$ -simplexes which has more than  $n + 1$  vertices such as the discrete simplexes of P4a and P8 for the 6-neighborhood system in Table 2. In mathematics such as combinatorial topology, simplexes are sometimes more

---

<sup>6</sup> For the proof that the 23 configurations are complete, see in the appendix B of [16]. Note that there are 22 configurations in [16] because symmetry is also considered.

focused on than cells or convex polyhedra. It is because polygonal 2-polyhedra are too general compared with triangular 2-simplexes. In our case, however, if we only use discrete simplexes for triangulation of a subset  $\mathbf{V}$  of  $\mathcal{Z}^3$ , the simplicial decomposition of  $\mathbf{V}$  may not be accomplished for 18-neighborhood system even if it is accomplished for 6- and 26-neighborhood systems [11]. In this paper, therefore, we show that triangulation of  $\mathbf{V}$  is succeeded for any neighborhood system by using not only discrete simplexes but also discrete convex polyhedra in Table 2.

### 3.3 Combinatorial Boundaries as Discrete Polyhedral Complexes

Before defining combinatorial boundaries, we give some topological notions for discrete polyhedral complexes [3]. A discrete  $n$ -complex  $\mathbf{K}$  is said to be *pure* if every discrete  $n'$ -polyhedron of  $\mathbf{K}$  where  $n' < n$  is a face of some discrete  $n$ -polyhedron. Figure 4 illustrates examples of pure and non-pure discrete 3-polyhedra for the 26-neighborhood system. If  $\mathbf{K}_0$  is any subset of  $\mathbf{K}$ , the complex consisting of all the elements of  $\mathbf{K}_0$  and of all the elements of  $\mathbf{K}$  each of which is a face of at least one element of  $\mathbf{K}_0$  is called the *combinatorial closure*  $Cl(\mathbf{K}_0)$  of  $\mathbf{K}_0$  in  $\mathbf{K}$ .

We consider a discrete polyhedral complex  $\mathbf{C}$  as a topological representation of  $\mathbf{V} \subset \mathcal{Z}^3$ , i.e., as a topological space by topologizing  $\mathbf{V}$ ; note that we topologize  $\mathbf{V}$  but not the whole space of  $\mathcal{Z}^3$ . Because we require our boundary representation to contain the surface structures such as triangulated surfaces, we consider a pure discrete 3-subcomplex  $\mathbf{O} \subseteq \mathbf{C}$  and define the boundary  $\partial\mathbf{O}$  of  $\mathbf{O}$  for the *combinatorial boundary* of  $\mathbf{V}$ ; a procedure for obtaining  $\partial\mathbf{O}$  from  $\mathbf{V}$  will be presented in the next section. The notion of such combinatorial boundary  $\partial\mathbf{O}$  is based on algebraic topology [28].

**Definition 3** *Let  $\mathbf{O}$  be a pure discrete 3-complex and  $\mathbf{H}$  be the set of all discrete 2-polyhedra in  $\mathbf{O}$  each of which is a face of exactly one discrete 3-polyhedron in  $\mathbf{O}$ . The boundary of  $\mathbf{O}$  is defined as*

$$\partial\mathbf{O} = Cl(\mathbf{H}).$$

From Definition 3, we obtain the following proposition.

**Proposition 4** *The boundary  $\partial\mathbf{O}$  of a pure discrete 3-complex  $\mathbf{O}$  is a pure discrete 2-subcomplex of  $\mathbf{O}$ .*

Note that the union of all discrete convex polyhedra in  $\partial\mathbf{O}$  may not form a manifold but form a non-manifold such as a pseudo-manifold [28] and a quasi-manifold [21] as shown in Figure 1 according to the definition.

Because discrete convex polyhedra are defined for each  $m$ -neighborhood system where  $m = 6, 18, 26$ , a discrete polyhedral complex  $\mathbf{C}$ , a discrete pure 3-polyhedron

$\mathbf{O}$  and the combinatorial boundary  $\partial\mathbf{O}$  are also defined for each  $m$ -neighborhood system. When we insist a  $m$ -neighborhood system considering for them, they are denoted by  $\mathbf{C}_m$ ,  $\mathbf{O}_m$  and  $\partial\mathbf{O}_m$  instead.

## 4 Combinatorial Boundary Extraction

This section presents a procedure for obtaining the boundary  $\partial\mathbf{O}_m$  of a pure discrete 3-complex  $\mathbf{O}_m$  from any finite set  $\mathbf{V} \subset \mathbb{Z}^3$  for each  $m = 6, 18, 26$ . The procedure is divided into three steps as shown in Figure 5: (I) decompose  $\mathbf{V}$  into discrete  $n$ -polyhedra where  $n = 0, 1, 2, 3$  such that those discrete  $n$ -polyhedra constitutes a discrete polyhedral complex  $\mathbf{C}_m$  (from (a) to (b) in Figure 5), (II) from  $\mathbf{C}_m$ , obtain a pure discrete 3-subcomplex  $\mathbf{O}_m \subseteq \mathbf{C}_m$  (from (b) to (c) in Figure 5), and (III) extract the boundary  $\partial\mathbf{O}_m$  of  $\mathbf{O}_m$  for each  $m$ -neighborhood system,  $m = 6, 18, 26$  (from (c) to (d) in Figure 5). After explaining such a procedure in subsection 4.1, we also presents a practical algorithm for obtaining  $\partial\mathbf{O}_m$  directly from  $\mathbf{V}$  in subsection 4.2.

### 4.1 Theory of the Procedure

#### 4.1.1 Step 1: Polyhedral Decomposition of $\mathbf{V}$

The decomposition of  $\mathbf{V}$  into discrete convex polyhedra is achieved in two steps. For each  $x = (i, j, k)$  in  $\mathbb{Z}^3$ , let

$$\mathbf{D}(x) = \{(i + \varepsilon_1, j + \varepsilon_2, k + \varepsilon_3) \mid \varepsilon_i = 0 \text{ or } 1\}.$$

We say that the points of  $\mathbf{V}$  are 1-points and the points of  $\mathbb{Z}^3 \setminus \mathbf{V}$  are 0-points. For each  $x \in \mathbb{Z}^3$ , we locally consider a discrete polyhedral complex  $\mathbf{C}_m(x)$  as follows. If a discrete  $n$ -polyhedron  $\sigma$  for an  $m$ -neighborhood system exists with respect to an configuration of 1-points in  $\mathbf{D}(x)$  in Table 2, we set  $\mathbf{C}_m(x)$  to be a collection of  $\sigma$  and its faces where  $n = 0, 1, 2, 3$ . Otherwise, we consider discrete  $n$ -polyhedra  $\sigma$  such that  $n$  is as large as possible where  $n \leq 3$  and the vertices of  $\sigma$  are all 1-points in  $\mathbf{D}(x)$  and set  $\mathbf{C}_m(x)$  to be a collection of such  $\sigma$ s and their faces. For each 1-point configuration of  $\mathbf{D}(x)$ , we then obtain a discrete polyhedral complex  $\mathbf{C}_m(x)$  for each  $m = 6, 18, 26$  as shown in Tables 3, 4 and 5, respectively.

Now let

$$\mathbf{C}_m = \bigcup_{x \in \mathbb{Z}^3} \mathbf{C}_m(x) \tag{9}$$

and we verify that  $\mathbf{C}_m$  is mostly a discrete polyhedral complex satisfying the conditions in Definition 2; there are few exceptional cases that we need to replace  $\mathbf{C}_m(x)$ s in (9) to obtain a discrete polyhedral complex  $\mathbf{C}_m$  only for  $m = 18$ .

Say that  $\mathbf{C}_m(x)$  and  $\mathbf{C}_m(y)$  are adjacent if  $\mathbf{D}(x) \cap \mathbf{D}(y) \neq \emptyset$ . Their adjacency types are classified into the following three

$$\#(\mathbf{D}(x) \cap \mathbf{D}(y)) = 1, 2 \text{ or } 4 \text{ (and never } 3)$$

where  $\#(A)$  represents the number of elements of the set  $A$ . The adjacency types and the conceivable polyhedral decomposition at the joint are illustrated in Table 6. For each adjacent pair of  $\mathbf{C}_m(x)$  and  $\mathbf{C}_m(y)$ , let

$$\mathbf{C}_m(x, y) = \mathbf{C}_m(x) \cup \mathbf{C}_m(y). \quad (10)$$

We then verify, from Tables 3, 4 and 5, that  $\mathbf{C}_m(x, y)$  is mostly a discrete polyhedral complex satisfying the conditions of Definition 2; only for  $m = 18$ , there are two exceptional cases that we need to replace both  $\mathbf{C}_m(x)$  and  $\mathbf{C}_m(y)$  in (10) to obtain a discrete polyhedral complex  $\mathbf{C}_m(x, y)$ .

First, let us consider the case of  $\#(\mathbf{D}(x) \cap \mathbf{D}(y)) = 1$ . As shown in the first line of Table 6, the common point  $z$  is either 1- or 0-point. If  $z$  is a 0-point (Case 1),  $\mathbf{C}_m(x)$  and  $\mathbf{C}_m(y)$  include no common discrete convex polyhedron. Thus, we simply obtain  $\mathbf{C}_m(x, y)$  by (10) as empty. If  $z$  is a 1-point (Case 2), both  $\mathbf{C}_m(x)$  and  $\mathbf{C}_m(y)$  include a common discrete 0-polyhedron  $\sigma_0$ . Let us introduce the notion of the *skeleton*  $Sk(\sigma)$  of a discrete convex polyhedron  $\sigma$  such as the set of all vertices of  $\sigma$  [3]. Then, we have  $Sk(\sigma_0) = \{z\}$ . Thus, we obtain a discrete 0-complex  $\mathbf{C}_m(x, y) = \{\sigma_0\}$  by (10).

In the case of  $\#(\mathbf{D}(x) \cap \mathbf{D}(y)) = 2$ , there are two common points  $z_1$  and  $z_2$  as shown in the second line of Table 6. Since each of  $z_1$  and  $z_2$  is either 1- or 0-point, there are three possible configurations of 1- and 0-points for the pair of  $z_1$  and  $z_2$ . If both  $z_1$  and  $z_2$  are 0-points (Case 1), both  $\mathbf{C}_m(x)$  and  $\mathbf{C}_m(y)$  include no common discrete polyhedron. Thus, we obtain  $\mathbf{C}_m(x, y)$  by (10) as empty. If either of  $z_1$  and  $z_2$  is 1-point (Case 2), the 1-point becomes the common 0-polyhedron  $\sigma$  in  $\mathbf{C}_m(x)$  and  $\mathbf{C}_m(y)$ . Thus, we obtain a discrete 0-complex  $\mathbf{C}_m(x, y) = \{\sigma\}$  by (10). If both  $z_1$  and  $z_2$  are 1-points (Case 3),  $\mathbf{C}_m(x)$  and  $\mathbf{C}_m(y)$  have a discrete 1-polyhedron  $\sigma$  and its 0-dimensional faces as the common discrete polyhedra such that  $Sk(\sigma) = \{z_1, z_2\}$ . Thus, we obtain a discrete 1-complex  $\mathbf{C}_m(x, y) = Cl(\{\sigma\})$  by (10).

In the case of  $\#(\mathbf{D}(x) \cap \mathbf{D}(y)) = 4$ , let  $z_i$  for  $i = 1, 2, 3, 4$  be the four common points. Since each point is either 1- or 0-point, there are six configurations of 1- and 0-points for the four points as shown in the last line of Table 6. It also shows the possible common discrete polyhedra of  $\mathbf{C}_m(x)$  and  $\mathbf{C}_m(y)$  for each configuration;

- the empty set in Case 1;

- a discrete 0-polyhedron  $\sigma_0$  such that  $Sk(\sigma_0) = \{z_2\}$  in Case 2;
- a discrete 1-polyhedron  $\sigma_1$  and its 0-dimensional faces such that  $Sk(\sigma_1) = \{z_2, z_3\}$  in Case 3;
- two discrete 0-polyhedra  $\sigma_{00}$  and  $\sigma_{01}$  such that  $Sk(\sigma_{00}) = \{z_2\}$  and  $Sk(\sigma_{01}) = \{z_4\}$  for the 6-neighborhood system and a discrete 1-polyhedron  $\sigma_1$  with its 0-dimensional faces such that  $Sk(\sigma_1) = \{z_2, z_4\}$  for the 18- and 26-neighborhood systems in Case 4;
- two discrete 1-polyhedra  $\sigma_{10}$  and  $\sigma_{11}$  with their faces such that  $Sk(\sigma_{10}) = \{z_2, z_3\}$  and  $Sk(\sigma_{11}) = \{z_3, z_4\}$  for the 6-neighborhood system, and a discrete 2-polyhedron  $\sigma_2$  with its faces such that  $Sk(\sigma_2) = \{z_2, z_3, z_4\}$  for the 18- and 26-neighborhood systems in Case 5;
- in Case 6, a discrete 2-polyhedron  $\sigma$  and its faces such that  $Sk(\sigma) = \{z_1, z_2, z_3, z_4\}$  for any neighborhood system except for the cases illustrated in Figures 6 (a) and (c) which appear only when  $m = 18$ .

We now discuss the exceptional cases which appear only for the 18-neighborhood system as illustrated in Figures 6 (a) and (c). In Figure 6 (a), both adjacent unit cubes  $\mathbf{D}(x)$  and  $\mathbf{D}(y)$  have the configurations P5a. In such case,  $\mathbf{C}_{18}(x)$  includes two discrete 2-polyhedra  $\sigma_{20}$  and  $\sigma_{21}$  such that  $Sk(\sigma_{20}) = \{z_1, z_2, z_3\}$  and  $Sk(\sigma_{21}) = \{z_1, z_4, z_3\}$ , and  $\mathbf{C}_{18}(y)$  includes two discrete 2-polyhedra  $\sigma_{22}$  and  $\sigma_{23}$  such that  $Sk(\sigma_{22}) = \{z_1, z_2, z_4\}$  and  $Sk(\sigma_{23}) = \{z_2, z_3, z_4\}$ . Thus, if  $\mathbf{C}_{18}(x, y)$  is obtained by (10), such  $\mathbf{C}_{18}(x, y)$  does not become a discrete polyhedral complex. In order to construct  $\mathbf{C}_{18}(x, y)$  which is a discrete polyhedral complex, we therefore replace discrete polyhedral complexes  $\mathbf{C}_{18}(x)$  and  $\mathbf{C}_{18}(y)$  from Figure 6 (a) to (b) so that

$$\begin{aligned}\mathbf{C}_{18}(x) &= Cl(\{\tau_{20}\}) \cup Cl(\{\tau_{21}\}), \\ \mathbf{C}_{18}(y) &= Cl(\{\tau_{22}\}) \cup Cl(\{\tau_{23}\})\end{aligned}$$

where  $Sk(\tau_{20}) = \{z_1, z_2, z_5\}$ ,  $Sk(\tau_{21}) = \{z_2, z_3, z_5\}$ ,  $Sk(\tau_{22}) = \{z_3, z_2, z_6\}$ , and  $Sk(\tau_{23}) = \{z_4, z_3, z_6\}$ . We then obtain

$$\begin{aligned}\mathbf{C}_{18}(x, y) &= \mathbf{C}_{18}(x) \cup \mathbf{C}_{18}(y) \\ &= Cl(\tau_{10}) \cup Cl(\tau_{11}) \cup Cl(\tau_{12})\end{aligned}$$

where  $Sk(\tau_{10}) = \{z_1, z_2\}$ ,  $Sk(\tau_{11}) = \{z_2, z_3\}$  and  $Sk(\tau_{12}) = \{z_3, z_4\}$ .

In Figure 6 (c), adjacent unit cubes  $\mathbf{D}(x)$  and  $\mathbf{D}(y)$  have the pair of configurations P5a and P4a. In such case,  $\mathbf{C}_{18}(x)$  includes two discrete 2-polyhedra  $\sigma_{20}$  and  $\sigma_{21}$  such that  $Sk(\sigma_{20}) = \{z_1, z_2, z_3\}$  and  $Sk(\sigma_{21}) = \{z_1, z_4, z_3\}$ , and  $\mathbf{C}_{18}(y)$  includes a discrete 2-polyhedron  $\sigma_{22}$  such that  $Sk(\sigma_{22}) = \{z_1, z_2, z_3, z_4\}$ . Thus, if  $\mathbf{C}_{18}(x, y)$  is obtained by (10), such  $\mathbf{C}_{18}(x, y)$  does not become a discrete polyhedral complex. In order to construct  $\mathbf{C}_{18}(x, y)$  which is a discrete polyhedral complex, we therefore replace discrete polyhedral complexes  $\mathbf{C}_{18}(x)$  and  $\mathbf{C}_{18}(y)$  from Figure 6 (c) to (d) so that

$$\begin{aligned}\mathbf{C}_{18}(x) &= Cl(\{\tau_{30}\}) \cup Cl(\{\sigma_{21}\}), \\ \mathbf{C}_{18}(y) &= Cl(\{\sigma_{20}\}) \cup Cl(\{\sigma_{21}\})\end{aligned}$$

where  $Sk(\tau_{30}) = \{z_1, z_2, z_3, z_5\}$ . We then obtain

$$\begin{aligned}\mathbf{C}_{18}(x, y) &= \mathbf{C}_{18}(x) \cup \mathbf{C}_{18}(y) \\ &= \mathbf{C}_{18}(y) \\ &= Cl(\sigma_{20}) \cup Cl(\sigma_{21}).\end{aligned}$$

Consequently, setting  $\mathbf{C}_m(x)$  for each  $x \in \mathbb{Z}^3$  referring to Tables 3, 4 and 5 with taking account of the additional replacements of Figure 6 for  $m = 18$ , we uniquely obtain  $\mathbf{C}_m$  by (9) for any  $m = 6, 18, 26$  from any  $\mathbf{V} \subset \mathbb{Z}^3$ .

#### 4.1.2 Step 2: Construction of a Pure Discrete 3-Complex

Assume that the dimension of  $\mathbf{C}_m$  is three. Let  $\mathbf{G}$  to be the set of all discrete 3-polyhedra in  $\mathbf{C}_m$ . In order to obtain a pure discrete 3-complex  $\mathbf{O}_m$  from  $\mathbf{C}_m$ , we remove all discrete  $n$ -polyhedra which are not included in any discrete 3-polyhedra in  $\mathbf{C}_m$  for every  $n < 3$ , such that

$$\mathbf{O}_m = Cl(\mathbf{G}). \quad (11)$$

If  $\mathbf{C}_m$  is less than three dimensions,  $\mathbf{G}$  is empty and thus  $\mathbf{O}_m$  is also empty. This occurs when  $\mathbf{C}_m$  contains only discrete 0-, 1- and 2-polyhedra and have no discrete 3-polyhedron. We consider that  $\mathbf{C}_m \setminus \mathbf{O}_m$  each of whose element has less than three dimensions is caused by the limited resolution of a digital image. If we would like to change the dimensions of elements in  $\mathbf{C}_m \setminus \mathbf{O}_m$  into three, we may need to increase the resolution of a digital image at  $\mathbf{C}_m \setminus \mathbf{O}_m$ . This is natural because our aim is to obtain surface structures from border points to calculate the shape information such as surface areas and curvatures. In order to obtain surface structures, apparently an isolated point is not adequate and we need to increase the image resolution to have more points around the isolated point.

From (11), it is clear that  $\mathbf{O}_m$  is uniquely obtained from  $\mathbf{C}_m$ . Examples of the procedure for obtaining  $\mathbf{O}_{26}$  from  $\mathbf{C}_{26}$  are seen in Figures 4 (from (b) to (a)) and 5 (from (b) to (c)).

We can also obtain  $\mathbf{O}_m$  directly from  $\mathbf{V}$  without considering  $\mathbf{C}_m$  such that

$$\mathbf{O}_m = \bigcup_{x \in \mathbb{Z}^3} \mathbf{O}_m(x)$$



where  $\mathbf{O}_m(x)$  is a pure discrete 3-complex at each unit cubic region  $\mathbf{D}(x)$ . Each  $\mathbf{O}_m(x)$  is easily obtained by referring to one of Tables 7, 8 and 9 instead of one of Tables 3, 4 and 5 for  $\mathbf{C}_m(x)$ . We easily create Tables 7, 8 and 9 by making  $\mathbf{C}_m(x)$  in Tables 3, 4 and 5 to be pure. Note that  $\mathbf{O}_{18}(x)$  will be replaced as an empty set if the 1-point configurations at  $\mathbf{D}(x)$  and its adjacent  $\mathbf{D}(y)$  are as illustrated in Figure 6 (a).

#### 4.1.3 Step 3: Boundary Extraction of a 3D Pure Discrete Complex

From Definition 3, the boundary  $\partial\mathbf{O}_m$  of  $\mathbf{O}_m$  is derived from the set  $\mathbf{H}$  of discrete 2-polyhedra in  $\mathbf{O}_m$  each of which is a face of exactly one discrete 3-polyhedron in  $\mathbf{O}_m$ . Because  $\mathbf{H}$  is uniquely obtained from  $\mathbf{O}_m$ ,  $\partial\mathbf{O}_m$  is also uniquely obtained from  $\mathbf{O}_m$ . From the above procedure, we consequently obtain the following proposition.

**Proposition 5** *Given a finite subset  $\mathbf{V} \subset \mathbb{Z}^3$ , the combinatorial boundary  $\partial\mathbf{O}_m$  is uniquely obtained for any  $m$ -neighborhood system,  $m = 6, 18, 26$ .*

#### 4.2 Algorithm of Combinatorial Boundary Extraction

For practical use, we present an effective algorithm of generating  $\partial\mathbf{O}_m$  directly from  $\mathbf{V}$  by referring to Table 10, which is a similar table used for the marching cubes method [22,32], for each neighborhood system. The comparison between the marching cubes method and our method is discussed in [12].

We obtain Table 10 from Tables 3, 4 and 5 as follows. First we look only for discrete 2-polyhedra of  $\mathbf{C}_m(x)$  at each unit cubic region  $\mathbf{D}_m(x)$  because  $\partial\mathbf{O}_m$  is a pure discrete 2-complex;  $\partial\mathbf{O}_m$  does not contain more than three-dimensional discrete convex polyhedra and less than two-dimensional discrete convex polyhedra which are not faces of any discrete 2-polyhedra. We then classify each discrete 2-polyhedron  $\sigma$  of  $\mathbf{C}_m(x)$  in Tables 3, 4 and 5 into the following four types, A-1, A-2, B-1, B-2:

A.  $\sigma$  is a face of a discrete 3-polyhedron  $\delta \in \mathbf{C}_m(x)$  so that

$$\sigma = \delta \cap \{x \in \mathcal{R}^3 : a \cdot x = z\} \quad (12)$$

where  $a \cdot x \leq z$  is valid for  $\delta$ , and

A-1.  $\sigma$  is located at a face of a unit cube  $\mathbf{D}(x)$  so that

$$\{x \in \mathcal{R}^3 : a \cdot x \leq z\} \cap \mathbf{D}(x) = \mathbf{D}(x); \quad (13)$$

A-2.  $\sigma$  is located inside a unit cube  $\mathbf{D}(x)$  so that (13) does not hold;

B.  $\sigma$  is not a face of any discrete 3-polyhedron  $\delta \in \mathbf{C}_m(x)$ , i.e., there is no discrete 3-polyhedron  $\delta$  which satisfies (12), and

B-1.  $\sigma$  is located at a face of a unit cube  $\mathbf{D}(x)$ , so that either of the equations

$$\{x \in \mathcal{R}^3 : a \cdot x \leq z\} \cap \mathbf{D}(x) = \mathbf{D}(x), \quad (14)$$

$$\{x \in \mathcal{R}^3 : a \cdot x \geq z\} \cap \mathbf{D}(x) = \mathbf{D}(x) \quad (15)$$

holds where

$$\sigma = \sigma \cap \{x \in \mathcal{R}^3 : a \cdot x = z\};$$

B-2.  $\sigma$  is located inside a unit cube  $\mathbf{D}(x)$  so that neither (14) nor (15) holds.

For each  $\mathbf{C}_m(x)$ , we obtain the set of discrete 2-polyhedra of each type, A-1, A-2, B-1, B-2, which is denoted by  $\mathbf{TP}_{11}(x)$ ,  $\mathbf{TP}_{12}(x)$ ,  $\mathbf{TP}_{21}(x)$  or  $\mathbf{TP}_{22}(x)$ , respectively. In the following, we show that only two types  $\mathbf{TP}_{12}(x)$  and  $\mathbf{TP}_{21}(x)$  can be found in  $\partial\mathbf{O}_m$ .

For  $\sigma \in \mathbf{TP}_{11}(x)$ ,  $\sigma$  does not belong to  $\partial\mathbf{O}_m$  if there exists a discrete 3-polyhedron  $\delta$  at a unit cube  $\mathbf{D}(y)$  adjacent to  $\mathbf{D}(x)$  such that  $\sigma$  is a face of  $\delta$ . If there is no such  $\delta$  at  $\mathbf{D}(y)$ , then  $\sigma \in \mathbf{TP}_{21}(y)$ . For  $\sigma \in \mathbf{TP}_{22}(x)$ ,  $\sigma \in \mathbf{C}_m \setminus \mathbf{O}_m$  and thus  $\sigma \notin \partial\mathbf{O}_m$ .

Setting

$$\mathbf{I}_m(x) = \bigcup_{\sigma \in \mathbf{TP}_{12}(x)} Cl(\sigma), \quad (16)$$

$$\mathbf{J}_m(x) = \bigcup_{\sigma \in \mathbf{TP}_{21}(x)} Cl(\sigma), \quad (17)$$

in Table 10 we obtain a pure discrete 2-complex

$$\mathbf{T}_m(x) = \mathbf{J}_m(x) \cup \mathbf{I}_m(x). \quad (18)$$

for every  $x \in \mathcal{Z}^3$ . The arrow of every  $\sigma$  in Table 10 indicates the side where the half space  $\{x \in \mathcal{R}^3 : a \cdot x > z\}$  exists; roughly speaking, it is oriented to the exterior of  $\partial\mathbf{O}_m$  and is useful for visualization as a normal vector of each  $\sigma$ . Note that either  $\mathbf{J}_m(x)$  or  $\mathbf{I}_m(x)$  is empty for any  $\mathbf{T}_m(x)$  in Table 10 except for the configuration P5a of the 18-neighborhood system.

We then see that any  $\tau \in \mathbf{I}_m(x)$  constitutes  $\partial\mathbf{O}_m$ , thus,

$$\mathbf{I}_m(x) \subset \partial\mathbf{O}_m. \quad (19)$$

For a discrete 2-polyhedron  $\sigma \in \mathbf{J}_m(x)$ , if  $\sigma \in \mathbf{J}_m(y)$  at an adjacent unit cube  $\mathbf{D}(y)$  to  $\mathbf{D}(x)$  as shown in Figure 7, then

$$\sigma \in \mathbf{C}_m \setminus \mathbf{O}_m, \quad (20)$$

and otherwise

$$\sigma \in \partial\mathbf{O}_m. \quad (21)$$

Therefore, we need to verify (21) (or (20)) for each  $\sigma \in \mathbf{J}_m(x)$  for constructing  $\partial\mathbf{O}_m$ , while every  $\sigma \in \mathbf{I}_m(x)$  is always in  $\partial\mathbf{O}_m$  from (19). Such verification is achieved in step 2.3 in Algorithm 1. The special treatment for the cases illustrated in Figures 6 (a) and (c) which occur only for the 18-neighborhood system is also considered in step 2.2 in Algorithm 1. For the algorithm, we set an input lattice space to be finite such as

$$\mathbf{W} = \{(i, j, k) \in \mathbb{Z}^3 : 1 \leq i \leq L, 1 \leq j \leq M, 1 \leq k \leq N\}.$$

### Algorithm 1

**input:** A subset  $\mathbf{V}$  of  $\mathbf{W}$ .

**output:** A combinatorial boundary  $\partial\mathbf{O}_m$ .

**begin**

1 set  $m = 6, 18$  or  $26$ ;

2 **for each**  $x \in \mathbf{W}$  **do**

2.1 obtain  $\mathbf{T}_m(x)$  by referring to Table 10;

2.2 if  $m = 18$ , check if each pair of  $\mathbf{T}_m(x)$  and  $\mathbf{T}_m(y)$  for  $y = (i-1, j, k), (i, j-1, k), (i, j, k-1)$  where  $x = (i, j, k)$  is in the case as illustrated in Figure 6 (a) or (c); if so, replace  $\mathbf{T}_m(x)$  and  $\mathbf{T}_m(y)$  from Figure 6 (a) to (b), or (c) to (d);

2.3 if  $\mathbf{J}_m(x)$  of  $\mathbf{T}_m(x)$  is not empty, then check for each  $\sigma \in \mathbf{J}_m(x)$  if there exists  $y$  such that  $\sigma \in \mathbf{J}_m(y)$  where  $y = (i-1, j, k), (i, j-1, k), (i, j, k-1)$  as shown in Figure 7; if so, replace  $\mathbf{T}_m(x)$  and  $\mathbf{T}_m(y)$  with  $Cl(\mathbf{T}_m(x) \setminus Cl(\{\sigma\}))$  and  $Cl(\mathbf{T}_m(y) \setminus Cl(\{\sigma\}))$ ;

3 obtain  $\partial\mathbf{O}_m = \cup_{x \in \mathbf{W}} \mathbf{T}_m(x)$ .

**end**

From Algorithm 1, it is obvious that we obtain the combinatorial boundary  $\partial\mathbf{O}_m$  for each  $m = 6, 18, 26$  from any finite set  $\mathbf{V} \subset \mathbb{Z}^3$ .

Some experimental results of combinatorial boundaries  $\partial\mathbf{O}_m$  for the various inputs  $\mathbf{V}$ , such as digitized sphere, cube, torus and catenoid, with respect to  $m = 6, 18, 26$  are shown in Figures 8, 9, 10 and 11. Those inputs of volume data are made by Volgen [30].

## 5 Relations between Borders and Combinatorial Boundaries

We already introduced the notion of the skeleton  $Sk(\sigma)$  of a discrete convex polyhedron  $\sigma$  such as the set of the vertices of  $\sigma$  in the previous section [3]. Let  $\partial\mathbf{O}_m$  be the combinatorial boundary obtained by Algorithm 1 from a given  $\mathbf{V} \subset \mathbb{Z}^3$  for  $m = 6, 18, 26$ . We call the union of the skeletons of all discrete convex polyhedra of  $\partial\mathbf{O}_m$  the *skeleton* of  $\partial\mathbf{O}_m$  and it is denoted by  $Sk(\partial\mathbf{O}_m)$ . We then obtain the following relations between the skeleton  $Sk(\partial\mathbf{O}_m)$  and the border  $Br_{m'}(\mathbf{V})$  of (8). Those relations are considered to be the discrete version of the relation (5) in  $\mathcal{R}^3$ .

**Theorem 6** *The border  $Br_{m'}(\mathbf{V})$  and the skeleton  $Sk(\partial\mathbf{O}_m)$  of the combinatorial boundary  $\partial\mathbf{O}_m$  obtained from a finite subset  $\mathbf{V} \subset \mathbb{Z}^3$  have the relations such that*

$$Br_6(\mathbf{V}) = Sk(\partial\mathbf{O}_{26}) \cup (Sk(\mathbf{C}_{26}) \setminus Sk(\mathbf{O}_{26})) \quad (22)$$

$$= Sk(\partial\mathbf{O}_{18}) \cup (Sk(\mathbf{C}_{18}) \setminus Sk(\mathbf{O}_{18})) \setminus \mathbf{A}_{(6,18)}, \quad (23)$$

$$Br_{18}(\mathbf{V}) = Sk(\partial\mathbf{O}_6) \cup (Sk(\mathbf{C}_6) \setminus Sk(\mathbf{O}_6)) \setminus \mathbf{A}_{(18,6)}, \quad (24)$$

$$Br_{26}(\mathbf{V}) = Sk(\partial\mathbf{O}_6) \cup (Sk(\mathbf{C}_6) \setminus Sk(\mathbf{O}_6)). \quad (25)$$

where

$$\mathbf{A}_{(m',m)} = \bigcup_{x \in \mathbb{Z}^3} \mathbf{A}_{(m',m)}(x)$$

so that  $\mathbf{A}_{(m',m)}(x)$  is shown in the right column of Table 11 as the set of black points at a unit cube  $\mathbf{D}(x)$  only when  $\mathbf{D}(x)$  has a 1-point configuration P5a or P7 only for  $(m',m) = (6,18)$  or  $(18,6)$ , respectively. Note that  $\mathbf{A}_{(6,18)}(x)$  for the configuration P5a is empty if it has no adjacent unit cube whose configuration is also P5a as shown in Figure 6 (b).

A pair  $(m',m)$  of neighborhood systems which is considered in Theorem 6 is  $(6,26)$ ,  $(6,18)$ ,  $(18,6)$  or  $(26,6)$  and similar pairs  $(m',m)$  are also seen in the relations between  $Br'_m(\mathbf{V})$  and its  $m$ -connectivity mentioned in section 2.2.1 [16,18].

From Theorem 6, we can derive the following corollary which has more similar formulas to (5) for  $\mathcal{R}^n$  shown in [23].

**Corollary 7** *For a pure discrete 3-complex  $\mathbf{O}_m$  where  $m = 6, 18, 26$ , we have the relations such that*

$$Br_6(Sk(\mathbf{O}_{26})) = Sk(\partial\mathbf{O}_{26}),$$

$$Br_6(Sk(\mathbf{O}_{18})) = Sk(\partial\mathbf{O}_{18}) \setminus \mathbf{A}_{(6,18)},$$

$$Br_{18}(Sk(\mathbf{O}_6)) = Sk(\partial\mathbf{O}_6) \setminus \mathbf{A}_{(18,6)},$$

$$Br_{26}(Sk(\mathbf{O}_6)) = Sk(\partial\mathbf{O}_6).$$

To emphasize the difference between the continuous and discrete cases, however, we refer to the relations (22), (23), (24) and (25) of Theorem 6 rather than those of Corollary 7. The difference is that there is an additional term which is the second term for the union in the right side of each equation of (22), (23), (24) and (25) while there is no such additional term in (5). The second term  $Sk(\mathbf{C}_m) \setminus Sk(\mathbf{O}_m)$  is a set of vertices which are not included in any discrete 3-polyhedra but included in less than three-dimensional discrete convex polyhedra of  $\mathbf{C}_m$ . In Figure 5, we can see  $Sk(\mathbf{C}_m) \setminus Sk(\mathbf{O}_m)$  such as the right point which is included in a discrete 1-polyhedron in (b) but does not appear in (c). Because we have a step for removing less than three-dimensional parts from three-dimensional parts, namely, obtaining  $\mathbf{O}_m$  from  $\mathbf{C}_m$  such as a procedure from (b) to (c) in Figure 5, we need to have the second term  $Sk(\mathbf{C}_m) \setminus Sk(\mathbf{O}_m)$  to compare with the border points  $Br_{m'}(\mathbf{V})$  based on general topology. Note that not only discrete 1-polyhedra but also discrete 2- and 0-polyhedra may exist in  $\mathbf{C}_m \setminus \mathbf{O}_m$ . Therefore, for the 3-dimensional border extraction, we take account of three kinds of dimensions for removing the parts  $\mathbf{C}_m \setminus \mathbf{O}_m$  whose dimension are reduced, i.e. zero, one and two dimensions, while we have to take account of two kinds of dimensions, i.e. zero and one dimension, for the 2-dimensional border extraction. This difference causes the difficulty of 3-dimensional border tracking problem as we already mentioned in Subsection 2.2.1.

The third terms  $\mathbf{A}_{(6,18)}$  and  $\mathbf{A}_{(18,6)}$  which only appear in (23) and (24) respectively show the difference between  $Sk(\partial\mathbf{O}_{18})$  and  $Sk(\partial\mathbf{O}_{26})$  of (23) and (22) and the difference between  $Br_{18}(\mathbf{V})$  and  $Br_{26}(\mathbf{V})$  of (24) and (25), respectively. Note that  $\mathbf{A}_{(6,18)}$  rarely becomes non-empty;  $\mathbf{A}_{(6,18)}$  is not empty only if we have a pair of adjacent unit cubes whose 1-point configurations are both P5a as shown in Figure 6 (b).

For proving Theorem 6, we need the following two lemmas.

**Lemma 8** *For a unit cubic region  $\mathbf{D}(x)$ , setting*

$$CubeBr_{m'}(\mathbf{V};x) = \{y \in \mathbf{V} \cap \mathbf{D}(x) : \mathbf{D}(x) \cap \mathbf{N}_{m'}(y) \cap \bar{\mathbf{V}} \neq \emptyset\} \quad (26)$$

for each  $m' = 6, 18, 26$ , we have

$$Br_{m'}(\mathbf{V}) = \bigcup_{x \in \mathbb{Z}^3} CubeBr_{m'}(\mathbf{V};x). \quad (27)$$

**Proof.** Since

$$\mathbf{N}_{m'}(y) \cap \bar{\mathbf{V}} = \bigcup_{x \in \mathbb{Z}^3} (\mathbf{D}(x) \cap \mathbf{N}_{m'}(y) \cap \bar{\mathbf{V}}),$$

we obtain (27) from (8) and (26).  $\square$

The points in  $CubeBr_{m'}(\mathbf{V};x)$  are illustrated for every possible configuration of 1-points in  $\mathbf{D}(x)$  in Table 11.

**Lemma 9** *At each unit cubic region  $\mathbf{D}(x)$  for  $x \in \mathbb{Z}^3$ , setting  $\mathbf{T}_m(x)$  to be a discrete 2-complex given by Table 10,  $\mathbf{C}_m(x)$  to be a discrete polyhedral complex given by Tables 3, 4 and 5, and  $\mathbf{O}_m(x)$  to be a pure discrete 3-complex of  $\mathbf{C}_m(x)$  by Tables 7, 8 and 9, we have*

$$\begin{aligned} & Sk(\partial\mathbf{O}_m) \cup (Sk(\mathbf{C}_m) \setminus Sk(\mathbf{O}_m)) \\ &= \bigcup_{x \in \mathbb{Z}^3} (Sk(\mathbf{T}_m(x)) \cup (Sk(\mathbf{C}_m(x)) \setminus Sk(\mathbf{O}_m(x)) \setminus Sk(\mathbf{T}_m(x))))). \end{aligned} \quad (28)$$

**Proof.**

(I) First we show the following inclusion:

$$\begin{aligned} & \bigcup_{x \in \mathbb{Z}^3} (Sk(\mathbf{T}_m(x)) \cup (Sk(\mathbf{C}_m(x)) \setminus Sk(\mathbf{O}_m(x)) \setminus Sk(\mathbf{T}_m(x)))) \\ & \subset Sk(\partial\mathbf{O}_m) \cup (Sk(\mathbf{C}_m) \setminus Sk(\mathbf{O}_m)). \end{aligned} \quad (29)$$

Let us consider the two pure discrete 2-complexes  $\mathbf{J}_m(x)$  and  $\mathbf{I}_m(x)$  of (16) and (17) for each  $\mathbf{T}_m(x)$  of (18). From (18), we then derive the relation

$$Sk(\mathbf{T}_m(x)) = Sk(\mathbf{I}_m(x)) \cup Sk(\mathbf{J}_m(x)), \quad (30)$$

and from (19),

$$Sk(\mathbf{I}_m(x)) \subset Sk(\partial\mathbf{O}_m). \quad (31)$$

The point configurations of  $Sk(\mathbf{I}_m(x))$  are illustrated in Table 11. Let us consider a vertex  $z \in Sk(\mathbf{J}_m(x))$ . Because  $\mathbf{J}_m(x)$  is a pure discrete 2-complex, any  $z$  is included in a discrete 2-polyhedron  $\sigma \in \mathbf{J}_m(x)$  and such a  $\sigma$  satisfies either (20) or (21). If  $z$  is a vertex of  $\sigma$  of (20),

$$z \in Sk(\mathbf{C}_m) \setminus Sk(\mathbf{O}_m) \quad (32)$$

and if  $z$  is a vertex of  $\sigma$  of (21),

$$z \in Sk(\partial\mathbf{O}_m). \quad (33)$$

Thus,

$$Sk(\mathbf{J}_m(x)) \subset Sk(\partial\mathbf{O}_m) \cup (Sk(\mathbf{C}_m) \setminus Sk(\mathbf{O}_m)) \quad (34)$$

for any  $x \in \mathbb{Z}^3$ . The point configurations of  $Sk(\mathbf{J}_m(x))$  are also shown in Table 11. From (30), (31) and (34), we then obtain

$$Sk(\mathbf{T}_m(x)) \subset Sk(\partial\mathbf{O}_m) \cup (Sk(\mathbf{C}_m) \setminus Sk(\mathbf{O}_m)). \quad (35)$$

For each discrete convex polyhedron  $\sigma \in \mathbf{C}_m(x) \setminus \mathbf{O}_m(x) \setminus \mathbf{T}_m(x)$ , if  $\sigma \in \mathbf{T}_m(y)$  at other unit cube  $\mathbf{D}(y)$  adjacent to  $\mathbf{D}(x)$ , we have (20) or (21), and otherwise we have (20). Consequently, if a vertex  $z \in Sk(\mathbf{C}_m(x)) \setminus Sk(\mathbf{O}_m(x)) \setminus Sk(\mathbf{T}_m(x))$  is a vertex of  $\sigma$  of (21), we have (33), and if  $z$  is a vertex of  $\sigma$  of (20), we have (32). Thus,

$$\begin{aligned} & Sk(\mathbf{C}_m(x)) \setminus Sk(\mathbf{O}_m(x)) \setminus Sk(\mathbf{T}_m(x)) \\ & \subset Sk(\partial\mathbf{O}_m) \cup Sk(\mathbf{C}_m) \setminus Sk(\mathbf{O}_m) \end{aligned} \quad (36)$$

for any  $x \in \mathbb{Z}^3$ . The point configurations of  $Sk(\mathbf{C}_m(x)) \setminus Sk(\mathbf{O}_m(x)) \setminus Sk(\mathbf{T}_m(x))$  are also shown in Table 11.

From (35) and (36), we have

$$\begin{aligned} & Sk(\mathbf{T}_m(x)) \cup (Sk(\mathbf{C}_m(x)) \setminus Sk(\mathbf{O}_m(x)) \setminus Sk(\mathbf{T}_m(x))) \\ & \subset Sk(\partial\mathbf{O}_m) \cup (Sk(\mathbf{C}_m) \setminus Sk(\mathbf{O}_m)) \end{aligned}$$

for every  $x \in \mathbb{Z}^3$ , and thus we obtain the inclusion (29).

(II) Now we verify if there exists a point

$$z \in Sk(\partial\mathbf{O}_m) \cup (Sk(\mathbf{C}_m) \setminus Sk(\mathbf{O}_m))$$

such that

$$z \notin Sk(\mathbf{T}_m(x) \cup (Sk(\mathbf{C}_m(x)) \setminus Sk(\mathbf{O}_m(x)) \setminus Sk(\mathbf{T}_m(x)))) \quad (37)$$

for any  $x \in \mathbb{Z}^3$ . Considering a point  $z \in \mathbf{V} \cap \mathbf{D}(x)$  which satisfies (37) for a point  $x \in \mathbb{Z}^3$ , we see that

$$z \in Sk(\mathbf{O}_m) \setminus Sk(\partial\mathbf{O}_m)$$

from Tables 3, 4, 5, and Tables 10 and 11, namely,

$$z \notin Sk(\partial\mathbf{O}_m) \cup (Sk(\mathbf{C}_m) \setminus Sk(\mathbf{O}_m))$$

because

$$\begin{aligned} Sk(\mathbf{C}_m) &= (Sk(\partial\mathbf{O}_m) \cup (Sk(\mathbf{C}_m) \setminus Sk(\mathbf{O}_m))) \cup (Sk(\mathbf{O}_m) \setminus Sk(\partial\mathbf{O}_m)) \\ &= \mathbf{V} \end{aligned}$$

and

$$(Sk(\partial\mathbf{O}_m) \cup (Sk(\mathbf{C}_m) \setminus Sk(\mathbf{O}_m))) \cap (Sk(\mathbf{O}_m) \setminus Sk(\partial\mathbf{O}_m)) = \emptyset.$$

Therefore, if  $z \in Sk(\partial\mathbf{O}_m) \cup (Sk(\mathbf{C}_m) \setminus Sk(\mathbf{O}_m))$ , then

$$z \in Sk(\mathbf{T}_m(x) \cup (Sk(\mathbf{C}_m(x)) \setminus Sk(\mathbf{O}_m(x)) \setminus Sk(\mathbf{T}_m(x))))$$

and it contradicts (37).

From (I) and (II), we thus obtain (28).  $\square$

**Proof of Theorem 6.** For  $(m', m) = (6, 26), (26, 6)$ , we have

$$\begin{aligned} & CubeBr_{m'}(\mathbf{V}; x) \\ &= Sk(\mathbf{T}_m(x)) \cup (Sk(\mathbf{C}_m(x)) \setminus Sk(\mathbf{O}_m(x)) \setminus Sk(\mathbf{T}_m(x))) \end{aligned} \quad (38)$$

for any  $x \in \mathbb{Z}^3$  from (30) and Table 11. Thus, from Lemmas 8 and 9, we obtain (22) and (25).

For  $(m', m) = (6, 18)$ , if we have the case as shown in Figure 6 (b) for the configuration P5a of  $\mathbf{D}(x)$ , we see that

$$\begin{aligned} & CubeBr_{m'}(\mathbf{V}; x) \\ &= Sk(\mathbf{T}_m(x)) \cup (Sk(\mathbf{C}_m(x)) \setminus Sk(\mathbf{O}_m(x)) \setminus Sk(\mathbf{T}_m(x))) \setminus \mathbf{A}_{(6,18)}(x) \end{aligned}$$

from Table 11, and otherwise we have (38). Thus, we obtain (23).

For  $(m', m) = (18, 6)$ , for the configuration P7 of  $\mathbf{D}(x)$ , we see that

$$\begin{aligned} & CubeBr_{m'}(\mathbf{V}; x) \\ &= Sk(\mathbf{T}_m(x)) \cup (Sk(\mathbf{C}_m(x)) \setminus Sk(\mathbf{O}_m(x)) \setminus Sk(\mathbf{T}_m(x))) \setminus \mathbf{A}_{(18,6)}(x) \end{aligned}$$

from Table 11, and otherwise we have (38). Thus, we obtain (24).  $\square$

## 6 Conclusions and Discussions

In this paper, we gave a solution to one of the important problems in three-dimensional image analysis; “is it possible to give a triangulation of border points  $Br_m(\mathbf{V})$  such that all vertices of triangulated surfaces are border points and adjacent vertices are  $m$ -neighboring for  $m = 6, 18, 26$ ?” Our answer is “yes.” We also succeed to present Algorithm 1 which gives such a triangulated surface  $\partial\mathbf{O}_m$  from any finite subset  $\mathbf{V} \subset \mathbb{Z}^3$ . We insists that the calculation time is linear to the size of  $\mathbf{V}$ , i.e. the size of a 3-dimensional digital image, and it is the same as that of the set operation



(8) for obtaining  $Br_m(\mathbf{V})$  from  $\mathbf{V}$  even if our algorithm provides a pure discrete 2-polyhedron  $\partial\mathbf{O}_m$  which contains not only a point set  $Sk(\partial\mathbf{O}_m)$  but also the combinatorial topological structures of  $\partial\mathbf{O}_m$ . Theorem 6 which indicates discrete versions of the relation (5) shows that  $\partial\mathbf{O}_{m'}$  becomes a triangulation of  $Br_m(\mathbf{V})$  if we choose a good pair such as  $(m, m') = (6, 18), (6, 26), (18, 6), (26, 6)$ . Note that there may be extra points of  $Sk(\mathbf{C}_{m'}) \setminus Sk(\mathbf{O}_{m'})$  if  $Br_m(\mathbf{V})$  contains some lattice points where we cannot put any discrete 3-polyhedron because of their configurations such as the configuration around the right point of Figure 5 (b). Our discrete polyhedral complex is useful to analyse the reasons why we have to ignore such points, i.e. points of  $Sk(\mathbf{C}_{m'}) \setminus Sk(\mathbf{O}_{m'})$  for triangulation of  $Br_m(\mathbf{V})$ . It is also interesting that the possible pairs for  $(m, m')$  are similar to the pairs  $(\alpha, \beta)$  for  $\beta$ -connectedness of  $\alpha$ -borders [18] as we mentioned in Section 2.2.1.

### 6.1 Improvement of the Combinatorial Boundary Tracking Algorithm

It may be also possible to present more effective combinatorial boundary tracking algorithms whose calculation time is linear to the number of border points if we succeed to investigate every possible local configurations of combinatorial boundaries. In fact, such an effective border tracking algorithm for three-dimensional digital image is already presented by using an algebraic-topology based approach by using voxel faces [21]. We only need to extend the algorithm for discrete polyhedral complexes instead of their cellular complexes.

### 6.2 Comparison with Other Polyhedral Complexes in $\mathbb{Z}^n$

We took the combinatorial/algebraic-topology based approach by using discrete polyhedral complexes for giving a solution to the triangulation problem. Due to the strong powers for topological problems in discrete spaces, similar simplicial representations for a finite subset  $\mathbf{V} \subset \mathbb{Z}^3$  are also seen in different literatures [14,18,29], for example. For our term of “discrete polyhedral complexes”  $\mathbf{C}_m$  for  $\mathbf{V}$ , they use the different terms: “cellular complexes” [14], “continuous analogs” [18] and “polyhedra” [29]. Because their aims are different, the ways of obtaining  $\mathbf{C}_m$  from  $\mathbf{V}$  are also different.

“Continuous analogs” are presented for defining a digital fundamental group whose concept is used for three-dimensional thinning. During three-dimensional thinning, they need to preserve a “digital topology” whose criteria are given by using the concepts of connectedness and of a digital fundamental group. For a digital fundamental group, they need to consider a region of interest and also its complement, and therefore consider topologies for the whole  $\mathbb{Z}^3$ , not only for  $\mathbf{V} \subset \mathbb{Z}^3$  as we do in this paper. In [18], one example for a set of continuous analogs is presented. They are different from our discrete polyhedral complexes in the geometric sense;

for example, some continuous analogs may have augmented points which are not lattice points but centroids of lattice cubes as their vertices. On the other hand, if we consider discrete polyhedral complexes  $\mathbf{C}_m(\mathbf{V})$  and  $\mathbf{C}_{m'}(\bar{\mathbf{V}})$  choosing some pairs for  $(m, m')$  for  $\mathbf{V}$  and  $\bar{\mathbf{V}}$ , then we do not know if they satisfy the conditions of continuous analogs or not. Because such discussion is beyond the subjects of this paper, we leave it for our future work.

Even if the aims in [14,29] are different from ours such as calculation of topological equivalence between two different subsets of  $\mathcal{Z}^3$  [29], we see that “cellular complexes” [14] and “polyhedra” [29] are the same as our discrete polyhedral complexes  $\mathbf{C}_6(\mathbf{V})$  for the 6-neighborhood system. This is because the shapes of discrete convex polyhedra for  $m = 6$  such as cubes, squares, unit line segments, etc. can be seen in lattice grids and they are straightforward to topologize  $\mathcal{Z}^3$ . In fact, if we topologize  $\mathcal{Z}^3$  instead of  $\mathbf{V} \subset \mathcal{Z}^3$  in the same way of  $\mathbf{C}_6(\mathbf{V})$ , i.e.  $\mathbf{C}_6(\mathcal{Z}^3)$ , we see Khalimsky space [13] which is well known in digital image analysis. In [15] it is also shown that Khalimsky space is homeomorphic to Kovalevsky’s finite topology [20] for the case  $\mathcal{Z}^2$ .

## Acknowledgements

A part of this work was done when the first author stayed at Laboratoire A2SI, ES-IEE, Cité Descartes, B.P. 99, 93162 Noisy-Le-Grand Cedex, France, with the support of the JSPS Postdoctoral Fellowships for Research Abroad from 2000 to 2002. She thanks Gilles Bertrand and Michel Couprie at ESIEE for useful discussion on the subject. Parts of the experiments were made by Yusuke Oda at Department of Information Technology, Okayama University.

## References

- [1] E. Andres, R. Acharya, C. Sibata, “Discrete Analytical Hyperplanes,” *Graphical Models and Image Processing*, Vol.59, No.5, pp.302–309, 1997.
- [2] E. Andres, M.-A. Jacob, “The Discrete Analytical Hyperspheres,” *IEEE Transactions on Visualization and Computer Graphics*, Vol.3, No.1, pp.75–86, 1997.
- [3] P. S. Alexandrov, *Combinatorial topology I*, Graylock Press: Rochester, 1956.
- [4] E. Artzy, G. Frieder, G. T. Herman, “The theory, design, implementation, and evaluation of a three-dimensional surface detection algorithm,” *Computer Graphics and Image Processing*, Vol. 15, pp. 1–24, 1981.
- [5] W. K. Clifford, “The postulates of the science of space”(1873), in *The world of mathematics Vol. 1*, J. R. Newman (Ed.), Simon & Schuster: New York, 1956, pp. 552–567.

- [6] M. Couprie, G. Bertrand, "Simplicity surfaces: a new definition of surfaces in  $\mathbf{Z}^3$ ," SPIE Vision Geometry VII, Vol. 3454, pp. 40–51, 1998.
- [7] I. Debled-Rennesson, J.-P. Reveilles, "A new approach to digital planes," SPIE Vision Geometry III, Vol.2356, pp.12–21, 1994.
- [8] J. Françon, "Discrete combinatorial surfaces," CVGIP: Graphical Models and Image Processing, Vol.57, No.1, pp.20–26, 1995.
- [9] F. Hausdorff, *Set Theory*, Chelsea Publishing Company: New York, 1937.
- [10] G. T. Herman, "Discrete multidimensional Jordan surfaces," CVGIP: Graphical Models and Image Processing, Vol. 54, No. 6, pp.507–515, 1992.
- [11] Y. Kenmochi, A. Imiya, A. Ichikawa, "Boundary extraction of discrete objects," Computer Vision and Image Understanding, Vol. 71, No. 3, pp. 281–293, 1998.
- [12] Y. Kenmochi, K. Kotani, A. Imiya, "Marching cubes method with connectivity," Proceedings of 1999 International Conference on Image Processing, Vol.4, pp.361–365, 1999.
- [13] E. Khalimsky, "Pattern analysis of N-dimensional digital images," Proceedings of IEEE International Conference on Systems, Man and Cybernetics, pp. 1559–1562, 1986.
- [14] R. Klette, "m-Dimensional cellular spaces," Technical Report CAR-TR-6, Center for Automation Research, University of Maryland, 1983.
- [15] R. Klette, "Digital Topology for Image Analysis, Part I; Basics and Planar Image Carriers," Technical Report CITR-TR-101, Center for Image Technology and Robotics, Tamaki Campus, The University of Auckland, 2001.
- [16] T. Y. Kong, A. W. Roscoe, "A Theory of Binary Digital Pictures," Computer Vision, Graphics, and Image Processing, Vol. 32, pp. 221–243, 1985.
- [17] T. Y. Kong, A. W. Roscoe, "Continuous Analogs of Axiomatized Digital Surfaces," Computer Vision, Graphics, and Image Processing, Vol. 29, pp. 60–86, 1985.
- [18] T. Y. Kong, A. W. Roscoe, A. Rosenfeld, "Concepts of digital topology," Topology and its Applications, Vol. 46, pp. 219–262, 1992.
- [19] T. Y. Kong, A. Rosenfeld, "Digital topology: introduction and survey," Computer Vision, Graphics, and Image Processing, Vol. 48, pp. 357–393, 1989.
- [20] V. A. Kovalevsky, "Finite topology as applied to image analyses," Computer Vision, Graphics, and Image Processing, Vol. 46, pp. 141–161, 1989.
- [21] V. A. Kovalevsky, "A topological method of surface representation," In Discrete Geometry for Computer Imagery, LNCS 1568, pp. 118–135, 1999.
- [22] W. E. Lorensen, H. E. Cline, "Marching cubes: a high-resolution 3d surface construction algorithm," Computer Graphics (SIGGRAPH '87), Vol. 21, No. 4, pp. 163–169, 1987.

- [23] E. E. Moise, *Geometric Topology in Dimensions 2 and 3*, Springer-Verlag: New York, 1977.
- [24] D. G. Morgenthaler, A. Rosenfeld, "Surfaces in three-dimensional images," *Information and Control*, Vol. 51, pp. 227–247, 1981.
- [25] A. Rosenfeld, "Connectivity in digital pictures," *Journal of the Association for Computing Machinery*, Vol. 17, No. 1, pp. 146–160, 1970.
- [26] F. Sloboda, B. Zařko, R. Klette, "On the topology of grid continua," In *Proc. Vision Geometry VII*, SPIE 3454, pp. 52–63, 1998.
- [27] P. Soille, *Morphological Image Analysis: Principles and Applications*, Springer: Berlin, 1999.
- [28] J. Stillwell, *Classical Topology and Combinatorial Group Theory*, Springer-Verlag: New York, 1993.
- [29] G. Tzurlakis, J. Mylopoulos, "Some results in computational topology," *Journal of the Association for Computing Machinery*, Vol.20, No.3, pp.439–455, 1973.
- [30] Volgen, [http://www.cb.uu.se/~tc18/code\\_data\\_set/Code/Volgen/](http://www.cb.uu.se/~tc18/code_data_set/Code/Volgen/)
- [31] K. Voss, *Discrete Images, Objects, and Functions in  $\mathbf{Z}^3$* , Springer-Verlag: Berlin, 1993.
- [32] G. Wyvill, G. McPheeters, B. Wyvill, "Data structure for *soft* objects," *The Visual Computer*, Vol. 2, pp. 227–234, 1986.
- [33] G. M. Ziegler, *Lectures on polytopes*, Springer-Verlag: New York, 1994.

## Figures

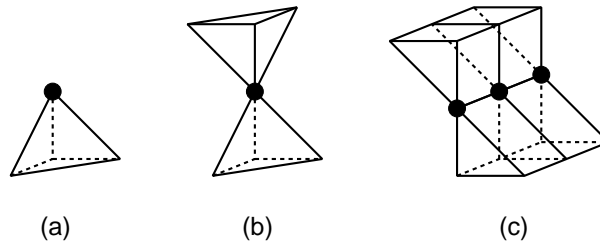


Fig. 1. Examples of manifolds and non-manifolds: (a) a manifold, (b) a pseudo-manifold [28], and (c) a quasi-manifold [21]. Each central black point is a border point which cannot be a point of simplicity surfaces [6].

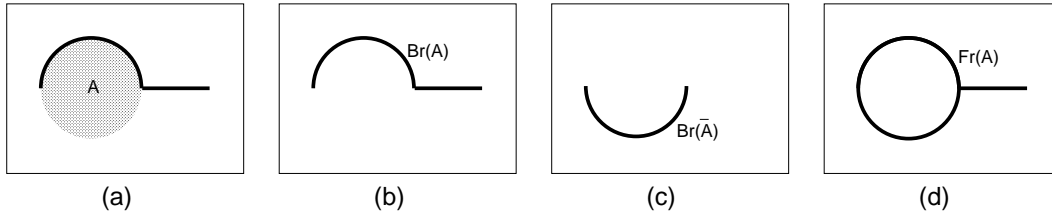


Fig. 2. Examples of (a) a point set  $\mathbf{A} \subset \mathcal{R}^2$ , (b) the border of  $\mathbf{A}$ , (c) the border of  $\bar{\mathbf{A}}$ , and (d) the frontier.

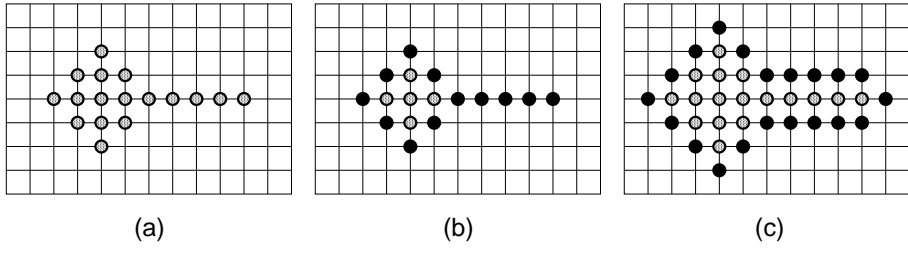


Fig. 3. Examples of (a) a point set  $V \subset \mathbb{Z}^2$ , (b) the 4-border of  $V$  and (c) the 4-border of  $\bar{V}$ .

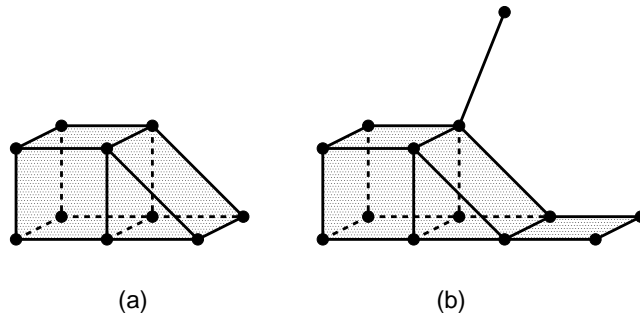


Fig. 4. Examples of (a) a pure discrete 3-polyhedron and (b) a non-pure discrete 3-polyhedron for the 26-neighborhood system.



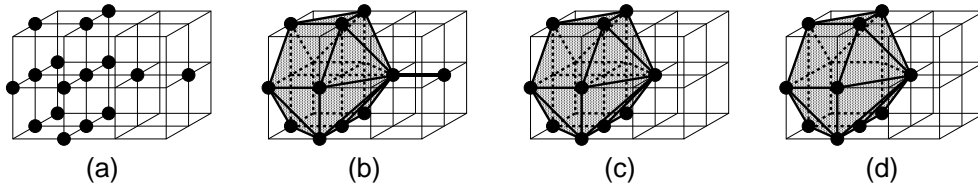


Fig. 5. The process of obtaining the boundary  $\partial\mathbf{O}_m$  of a pure discrete 3-complex  $\mathbf{O}_m$  from a finite subset  $\mathbf{V}$  of  $\mathbb{Z}^3$  via a discrete polyhedral complex  $\mathbf{C}_m$  for  $m = 6, 18, 26$ . The figures shows examples of (a) $\mathbf{V}$ , (b) $\mathbf{C}_{26}$ , (c) $\mathbf{O}_{26}$ , and (d) $\partial\mathbf{O}_{26}$ .

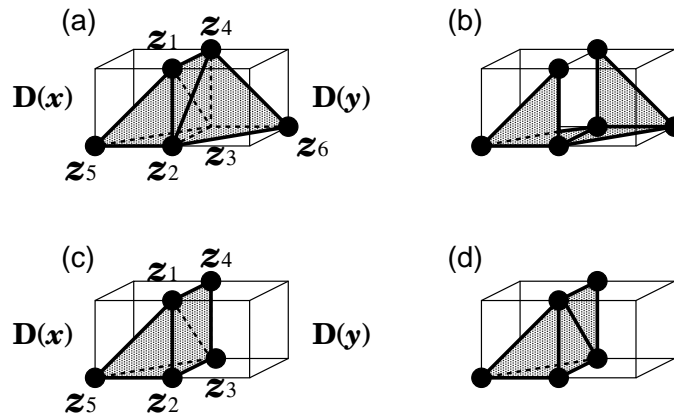


Fig. 6. Two cases (a) and (c) such that a union of two adjacent discrete polyhedral complexes which does not form a discrete polyhedral complex. We have such cases only when we consider the 18-neighborhood system. The case (a) occurs only if both the adjacent unit cubes have the 1-point configurations P5a. The case (c) occurs only if they have the 1-point configurations P5a and P4a. Polyhedral decompositions of (a) and (c) are replaced by those of (b) and (d), respectively.

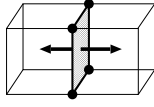
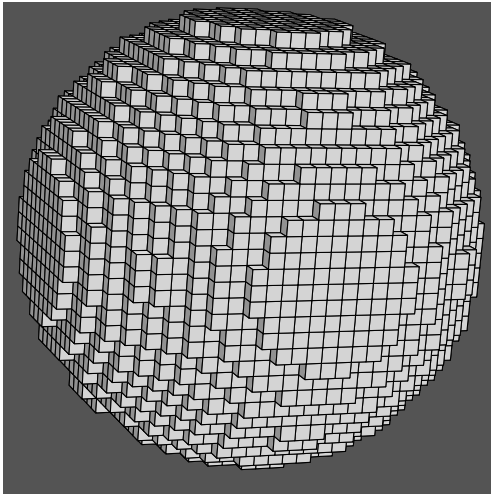
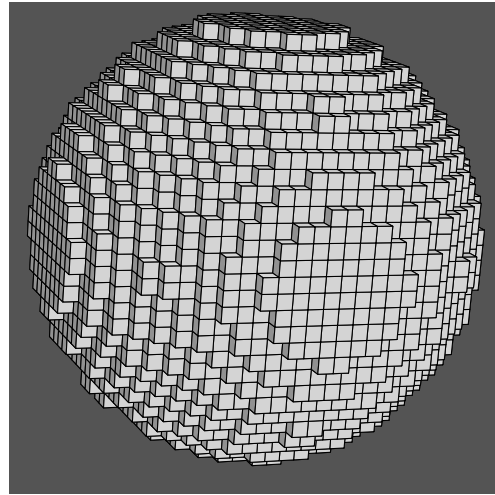


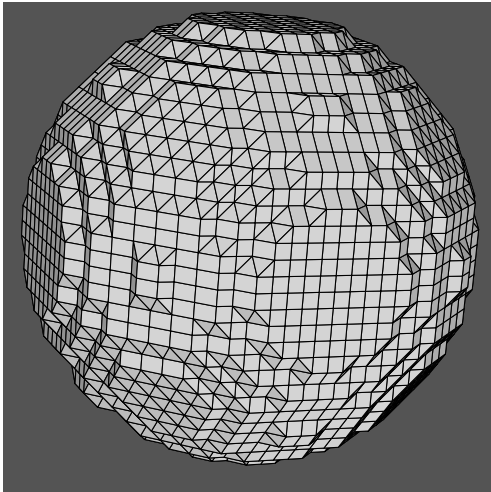
Fig. 7. An example of the case such that a common discrete 2-polyhedron  $\sigma$  exists in  $\mathbf{J}_m(x)$  and  $\mathbf{J}_m(y)$  at two adjacent unit cubes. Such  $\sigma$  does not constitute  $\partial\mathbf{O}_m$  but  $\mathbf{C}_m \setminus \mathbf{O}_m$ .



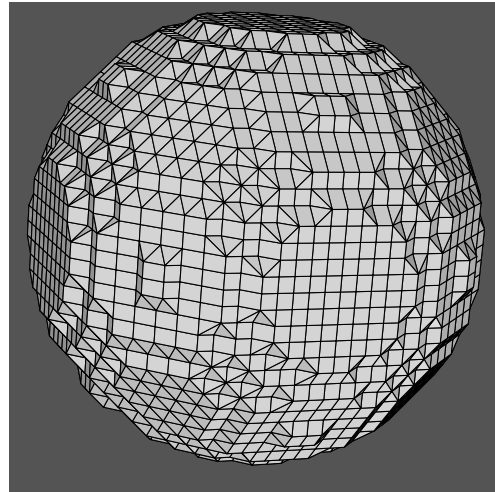
(a)



(b)



(c)



(d)

Fig. 8. (a) A digitized sphere generated by Volgen [30] and its combinatorial boundaries for (b) 6-, (c) 18- and (d) 26-neighborhood systems. Note that lattice points are located at centers of cubes in (a) whereas they are located at vertices of polyhedral complexes in (b), (c) and (d).

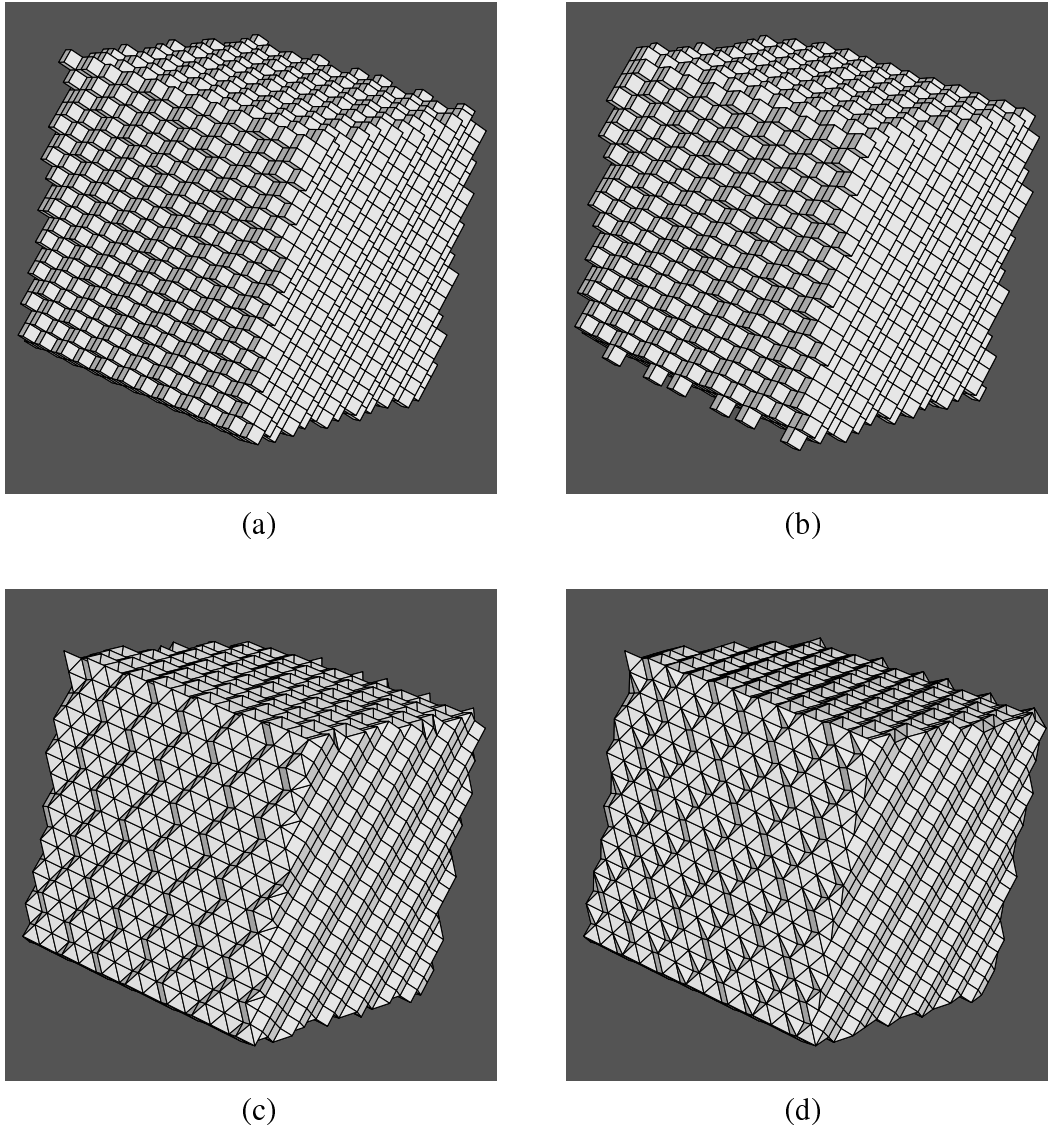


Fig. 9. (a) A digitized cube with 45-degree rotations around  $x$  and  $y$  axes, generated by Volgen [30], and its combinatorial boundaries for (b) 6-, (c) 18- and (d) 26-neighborhood systems. Note that lattice points are located at centers of cubes in (a) whereas they are located at vertices of polyhedral complexes in (b), (c) and (d).

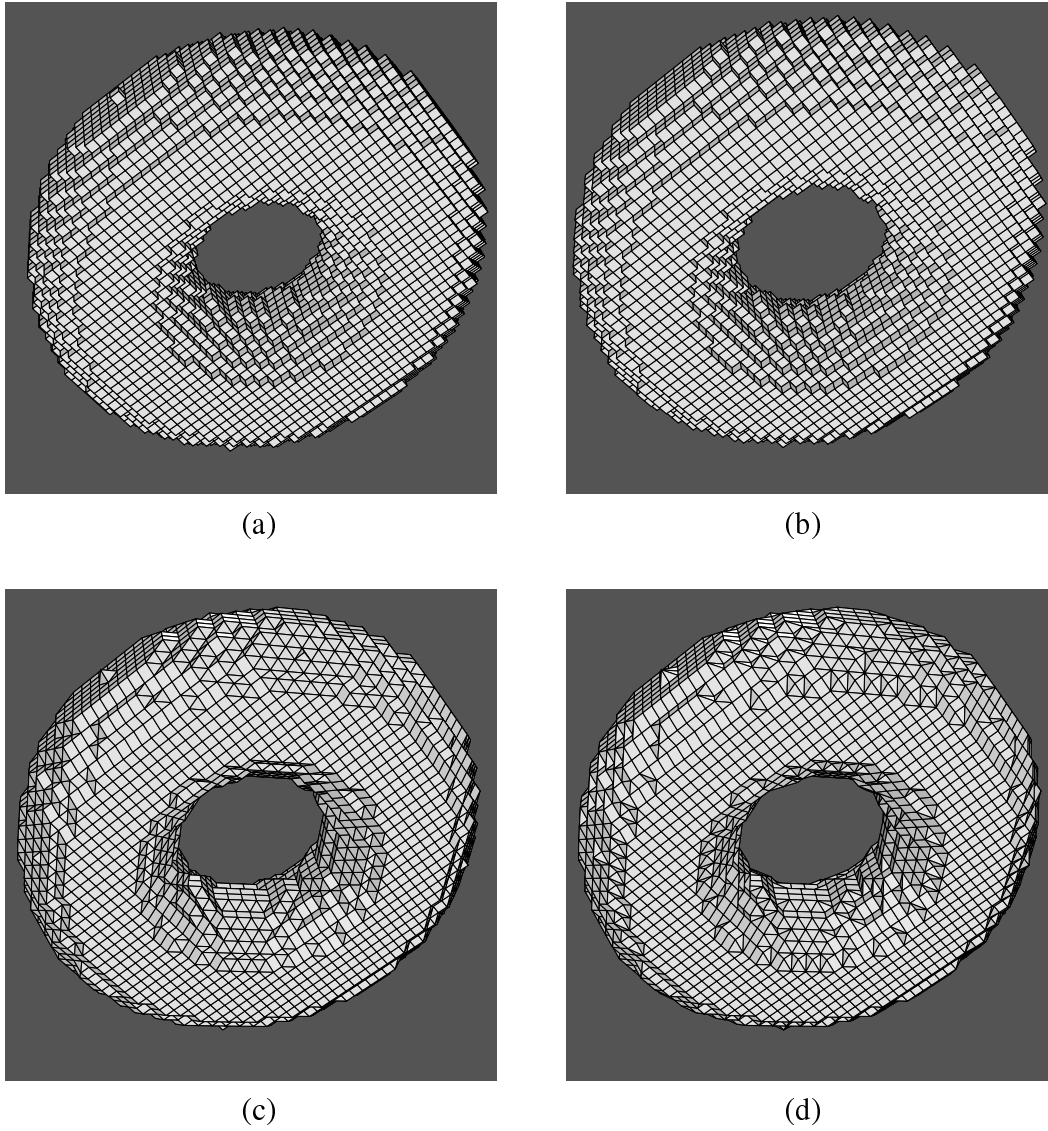
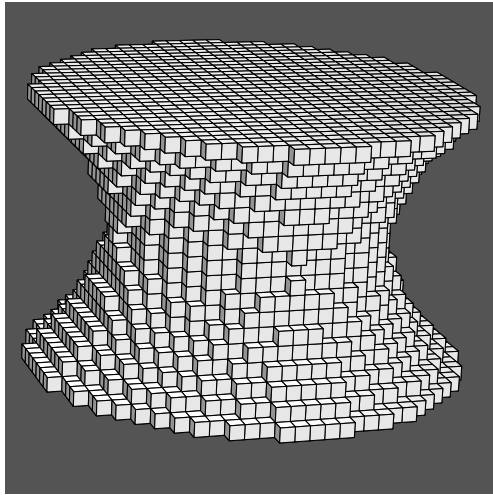
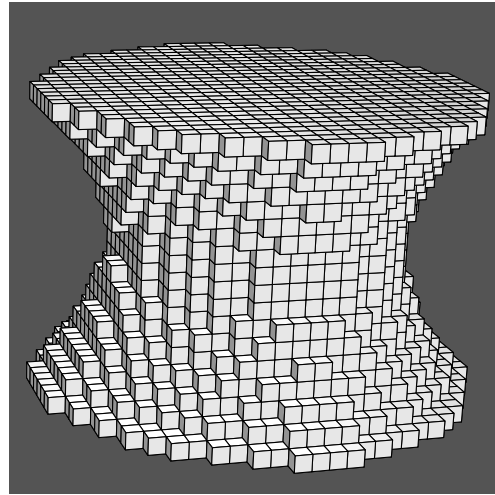


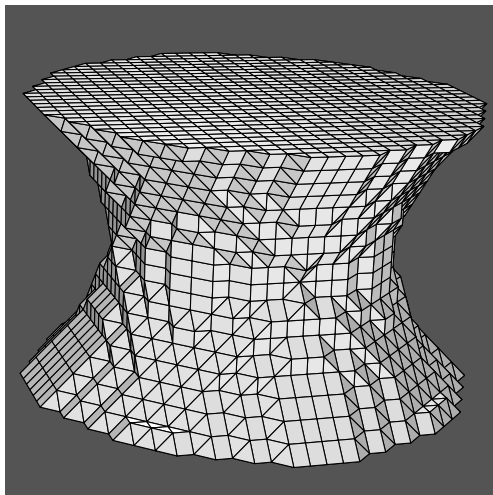
Fig. 10. (a) A digitized torus generated by Volgen [30], and its combinatorial boundaries for (b) 6-, (c) 18- and (d) 26-neighborhood systems. Note that lattice points are located at centers of cubes in (a) whereas they are located at vertices of polyhedral complexes in (b), (c) and (d).



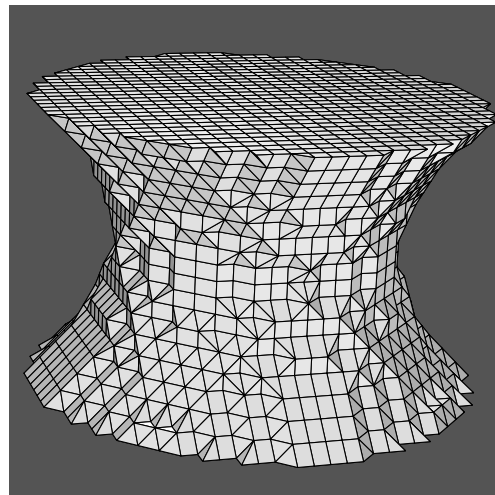
(a)



(b)



(c)



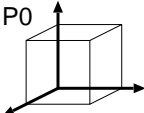
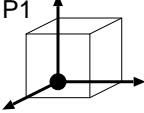
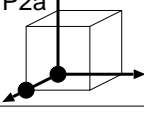
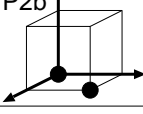
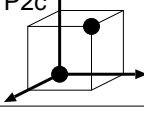
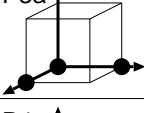
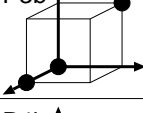
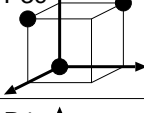
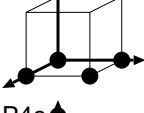
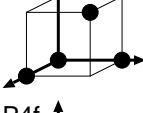
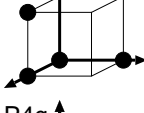
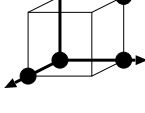
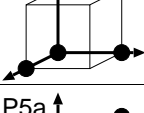
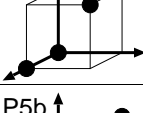
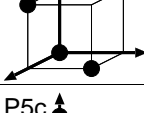
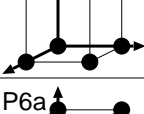
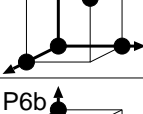
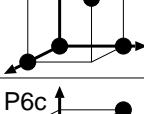
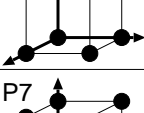
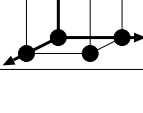
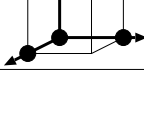
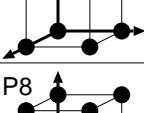
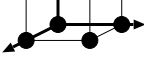
(d)

Fig. 11. (a) A digitized catenoid generated by Volgen [30], and its combinatorial boundaries for (b) 6-, (c) 18- and (d) 26-neighborhood systems. Note that lattice points are located at centers of cubes in (a) whereas they are located at vertices of polyhedral complexes in (b), (c) and (d).

## Tables

Table 1

All possible 23 configurations of 1- and 0-points for the eight lattice points in a unit cubic region. With considering the congruent configurations by rotations, we obtain all 256 configurations from them.

number of 1-points	configurations of 1- and 0-points in a unit cube
0	P0 
1	P1 
2	P2a  P2b  P2c 
3	P3a  P3b  P3c 
4	P4a  P4b  P4c  P4d  P4e  P4f  P4g 
5	P5a  P5b  P5c 
6	P6a  P6b  P6c 
7	P7 
8	P8 

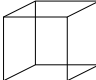

 a unit cube  
 a 1-point



Table 2

All discrete  $n$ -polyhedra for  $n = 0, 1, 2, 3$  such that all vertices are lattice points in  $\mathbb{Z}^3$  and the adjacent vertices are  $m$ -neighboring for  $m = 6, 18, 26$ . Note that discrete  $n$ -polyhedra with asterisks are called discrete  $n$ -simplexes in the reference [11].

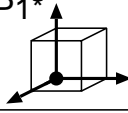
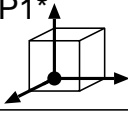
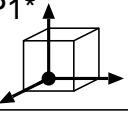
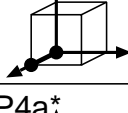

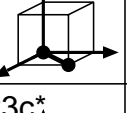
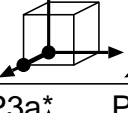
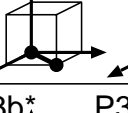
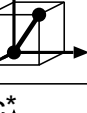
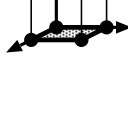

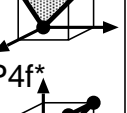
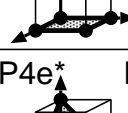
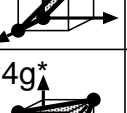
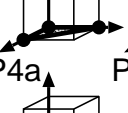
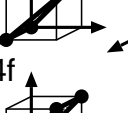
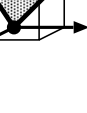
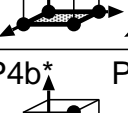
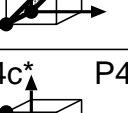
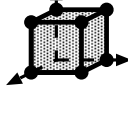




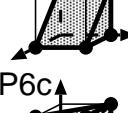
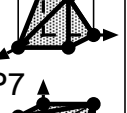
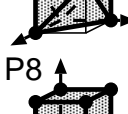



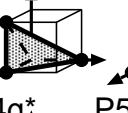


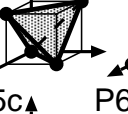




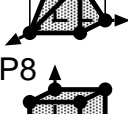



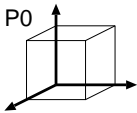
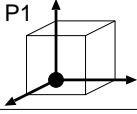
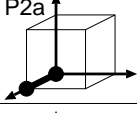
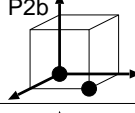
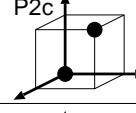
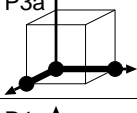
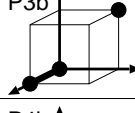
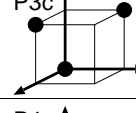
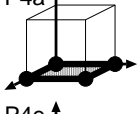
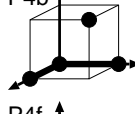
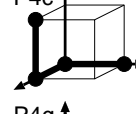
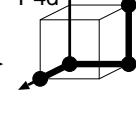
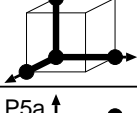
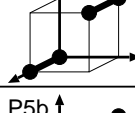
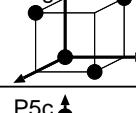
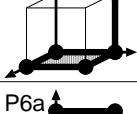
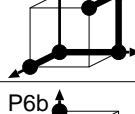
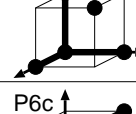
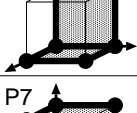
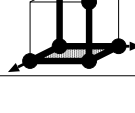
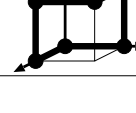
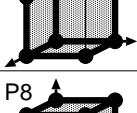

dim.	discrete convex polyhedra		
	N <sub>6</sub>	N <sub>18</sub>	N <sub>26</sub>
0	P1* 	P1* 	P1* 
1	P2a* 	P2a*  P2b* 	P2a*  P2b*  P2c* 
2	P4a* 	P3a*  P3c*  P4a  P4f* 	P3a*  P3b*  P3c*  P4a  P4f 
3	P8* 	P4e*  P4g*  P5b*  P5c  P6a  P6b  P6c  P7  P8 	P4b*  P4c*  P4d*  P4e*  P4g*  P5a  P5b  P5c  P6a  P6b  P6c  P7  P8 

Table 3

Discrete convex polyhedral decomposition  $C_6(x)$  with respect to every 1-point configuration of a unit cubic region  $D(x)$ .

# of 1-points	discrete convex polyhedral decomposition
0	P0 
1	P1 
2	P2a  P2b  P2c 
3	P3a  P3b  P3c 
4	P4a  P4b  P4c  P4d  P4e  P4f  P4g 
5	P5a  P5b  P5c 
6	P6a  P6b  P6c 
7	P7 
8	P8 



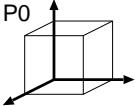
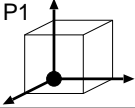
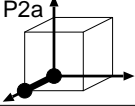
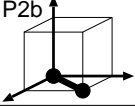
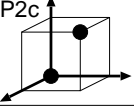
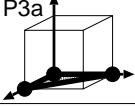
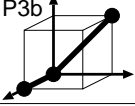
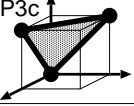
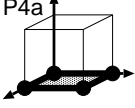
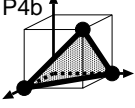
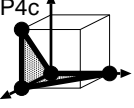
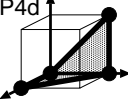
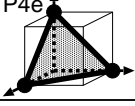
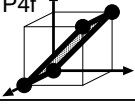
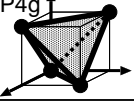
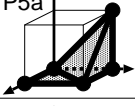
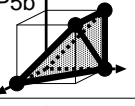
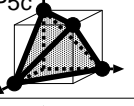
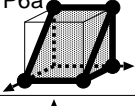
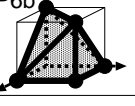
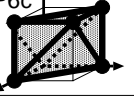


 a unit cube  
 a 1-point

Table 4

Discrete convex polyhedral decomposition  $C_{18}(x)$  with respect to every 1-point configuration of a unit cubic region  $D(x)$ .

# of 1-points	discrete convex polyhedral decomposition
0	P0 
1	P1 
2	P2a  P2b  P2c 
3	P3a  P3b  P3c 
4	P4a  P4b  P4c  P4d  P4e  P4f  P4g 
5	P5a  P5b  P5c 
6	P6a  P6b  P6c 
7	P7 
8	P8 

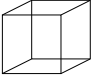

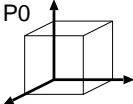
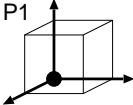
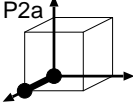
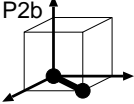
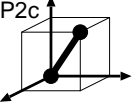
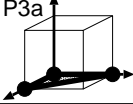
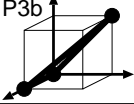
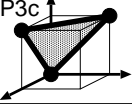
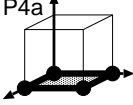

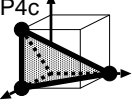
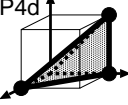
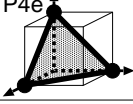
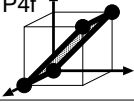
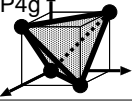


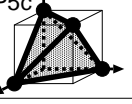
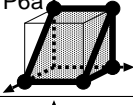
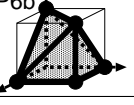
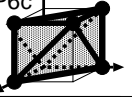


 a unit cube  
 a 1-point

Table 5  
 Discrete convex polyhedral decomposition  $C_{26}(x)$  with respect to every 1-point configuration of a unit cubic region  $D(x)$ .

# of 1-points	discrete convex polyhedral decomposition
0	P0 
1	P1 
2	P2a  P2b  P2c 
3	P3a  P3b  P3c 
4	P4a  P4b  P4c  P4d  P4e  P4f  P4g 
5	P5a  P5b  P5c 
6	P6a  P6b  P6c 
7	P7 
8	P8 

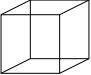

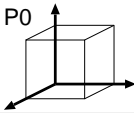
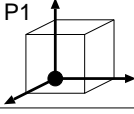
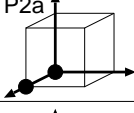
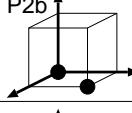
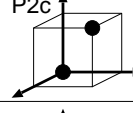
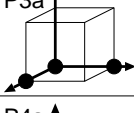
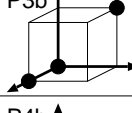
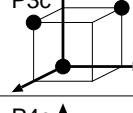
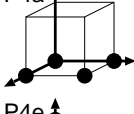
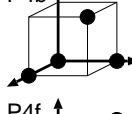
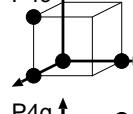
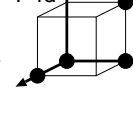
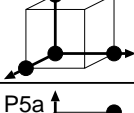
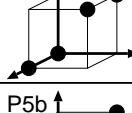
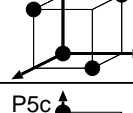
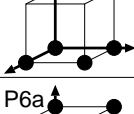
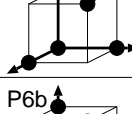
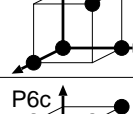
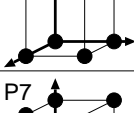
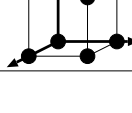
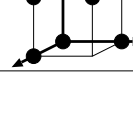

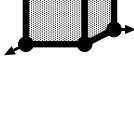
 a unit cube  
 a 1-point

Table 6

Three adjacency types of two unit cubic regions  $\mathbf{D}(x)$  and  $\mathbf{D}(y)$  such that  $\#\mathbf{D}(x) \cap \mathbf{D}(y) = 1, 2$  and  $4$ . For each adjacency type, all possible configurations of 1- and 0-points and a discrete convex polyhedral decomposition are shown.

$\#\mathbf{D}(x) \cap \mathbf{D}(y)$	cellular decomposition of $\mathbf{D}(x) \cap \mathbf{D}(y)$			
1	<p>Case 1</p>	<p>Case 2</p>	a unit cubic region	
2	<p>Case 1</p>	<p>Case 2</p>	<p>Case 3</p>	<ul style="list-style-type: none"> <li>● a 1-point</li> <li>○ a 0-point</li> </ul>
4	<p>Case 1</p>	<p>Case 2</p>	<p>Case 3</p>	
	<p>Case 4</p> <p><math>N_6</math></p>	<p>Case 5</p> <p><math>N_6</math></p>	<p>Case 6</p> <p><math>N_6</math> <math>N_{18}</math> <math>N_{26}</math></p>	
	<p>Case 4</p> <p><math>N_{18}</math> <math>N_{26}</math></p>	<p>Case 5</p> <p><math>N_{18}</math> <math>N_{26}</math></p>	<p>Case 6</p> <p><math>N_{18}</math> (P5a) <math>N_{18}</math> (P4a)</p>	

Table 7  
 Three-dimensional polyhedral decomposition  $\mathbf{O}_6(x)$  corresponding to the configuration of 1-points in a unit cubic region  $\mathbf{D}(x)$ .

# of 1-points	3D polyhedral decomposition			
0				
1				
2				
3				
4				
				
5				
6				
7				
8				

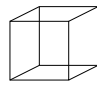

 a unit cube  
 a 1-point

Table 8  
 Three-dimensional polyhedral decomposition  $\mathbf{O}_{18}(x)$  corresponding to the configuration of 1-points in a unit cubic region  $\mathbf{D}(x)$ .

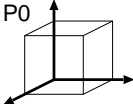
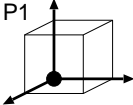
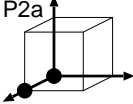
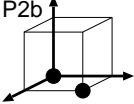
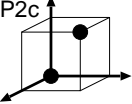
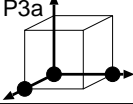
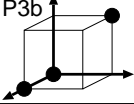
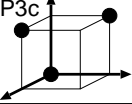
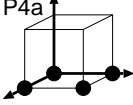
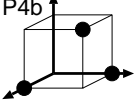
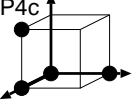
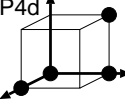
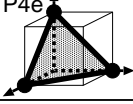
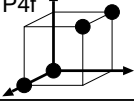
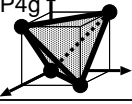
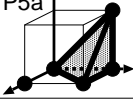

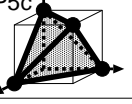
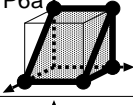
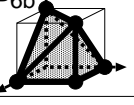
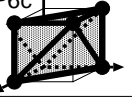


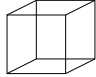

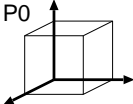
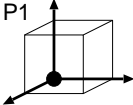
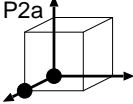
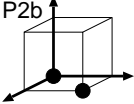
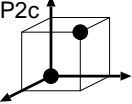
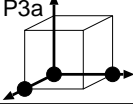
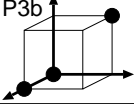
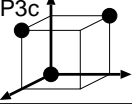
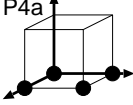

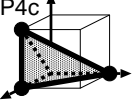
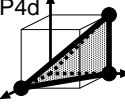
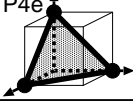
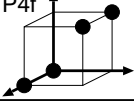
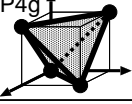


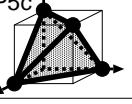
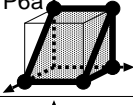
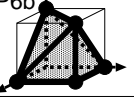
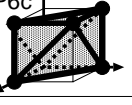


# of 1-points	3D polyhedral decomposition			
0				
1				
2				
3				
4				
				
5				
6				
7				
8				
				a unit cube
				a 1-point

Table 9  
 Three-dimensional polyhedral decomposition  $\mathbf{O}_{26}(x)$  corresponding to the configuration of 1-points in a unit cubic region  $\mathbf{D}(x)$ .

# of 1-points	3D polyhedral decomposition			
0				
1				
2				
3				
4				
				
5				
6				
7				
8				

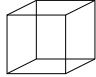

 a unit cube  
 a 1-point



Table 10

The look-up table which provides a one-to-one correspondence between an configuration of 1-points in a unit cubic region  $\mathbf{D}(x)$  and a pure discrete 2-complex  $\mathbf{T}_m(x)$  for the combinatorial boundary  $\partial\mathbf{O}_m$  of the set  $\mathbf{V}$  of all 1-points with respect to each  $m = 6, 18, 26$ . The arrows are oriented to the exterior of  $\partial\mathbf{O}_m$ .

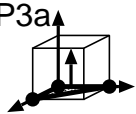


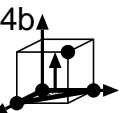

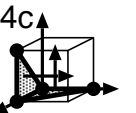

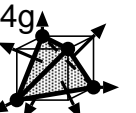








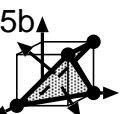



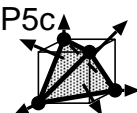

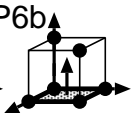

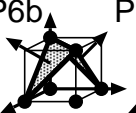
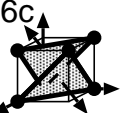


# of 1-points	2D pure subcomplex for a combinatorial boundary		
	N6	N18	N26
3		P3a 	
4	P4a 	P4a  P4b  P4d  P4c  P4e  P4g 	P4a  P4b  P4d  P4c  P4e  P4g 
5	P5a 	P5a  P5b  P5c 	P5a  P5b  P5c 
6	P6a  P6b 	P6a  P6b  P6c 	
7	P7 	P7 	

Table 11

For each 1-point configuration of a unit cube  $\mathbf{D}(x)$ , the configurations of points of  $CubeBr_{m'}(\mathbf{V};x)$  for  $m' = 6, 18, 26$ ,  $Sk(\mathbf{I}_m(x))$ ,  $Sk(\mathbf{J}_m(x))$  and  $Sk(\mathbf{C}_m(x)) \setminus Sk(\mathbf{O}_m(x)) \setminus Sk(\mathbf{T}_m(x))$  for  $m = 6, 18, 26$  are shown with  $\mathbf{A}_{(m',m)}(x)$  for the adjustment in the cases of  $(m', m) = (6, 18), (18, 6)$ .

1-point config.	$CubeBr_{m'}(\mathbf{V};x)$			$Sk(\mathbf{I}_m(x)), Sk(\mathbf{J}_m(x)), Sk(\mathbf{C}_m(x)) \setminus Sk(\mathbf{O}_m(x)) \setminus Sk(\mathbf{T}_m(x))$			$\mathbf{A}_{(m',m)}(x)$
	$m'=6$	$m'=18$	$m'=26$	$m=6$	$m=18$	$m=26$	
P0							
P1							
P2a							
P2b							
P2c							
P3a							
P3b							
P3c							
P4a							
P4b							
P4c							
P4d							
P4e							
P4f							
P4g							
P5a							$(m',m)=(6,18)$
P5b							
P5c							
P6a							
P6b							
P6c							
P7							$(m',m)=(18,6)$
P8							